

Normal variance mixtures: Distribution, density and parameter estimation

Erik Hintz¹, Marius Hofert², Christiane Lemieux³

2020-06-16

Abstract

Normal variance mixtures are a class of multivariate distributions that generalize the multivariate normal by randomizing (or mixing) the covariance matrix via multiplication by a non-negative random variable W . The multivariate t distribution is an example of such mixture, where W has an inverse-gamma distribution. Algorithms to compute the joint distribution function and perform parameter estimation for the multivariate normal and t (with integer degrees of freedom) can be found in the literature and are implemented in, e.g., the R package `mvtnorm`. In this paper, efficient algorithms to perform these tasks in the general case of a normal variance mixture are proposed. In addition to the above two tasks, the evaluation of the joint (logarithmic) density function of a general normal variance mixture is tackled as well, as it is needed for parameter estimation and does not always exist in closed form in this more general setup. For the evaluation of the joint distribution function, the proposed algorithms apply randomized quasi-Monte Carlo (RQMC) methods in a way that improves upon existing methods proposed for the multivariate normal and t distributions. An adaptive RQMC algorithm that similarly exploits the superior convergence properties of RQMC methods is presented for the task of evaluating the joint log-density function. In turn, this allows the parameter estimation task to be accomplished via an expectation-maximization-like algorithm where all weights and log-densities are numerically estimated. It is demonstrated through numerical examples that the suggested algorithms are quite fast; even for high dimensions around 1000 the distribution function can be estimated with moderate accuracy using only a few seconds of run time. Even log-densities around -100 can be estimated accurately and quickly. An implementation of all algorithms presented in this work is available in the R package `nvmix` (version $\geq 0.0.4$).

Keywords

Multivariate normal variance mixtures, distribution functions, densities, Student t , quasi-random number sequences.

¹Department of Statistics and Actuarial Science, University of Waterloo, 200 University Avenue West, Waterloo, ON, N2L 3G1, erik.hintz@uwaterloo.ca.

²Department of Statistics and Actuarial Science, University of Waterloo, 200 University Avenue West, Waterloo, ON, N2L 3G1, marius.hofert@uwaterloo.ca. The author would like to thank NSERC for financial support for this work through Discovery Grant RGPIN-5010-2015.

³Department of Statistics and Actuarial Science, University of Waterloo, 200 University Avenue West, Waterloo, ON, N2L 3G1, cllemieux@uwaterloo.ca. The author would like to thank NSERC for financial support for this work through Discovery Grant RGPIN-238959.

MSC2010

62H99, 65C60

1 Introduction

The multivariate normal and (Student) t distributions are among the most widely used multivariate distributions within applications in statistics, finance, insurance and risk management. A simple way to create a much larger range of distributions than the multivariate normal, with different (joint and marginal) tail behavior including tail dependence, is by randomizing (mixing) the covariance matrix of a multivariate normal distribution. This makes normal variance mixtures better suited, for example, for log-return distributions, while keeping many of the advantages of multivariate normal distributions such as closedness with respect to linear combinations; see McNeil et al. (2015, Section 6.2) for more details.

Formally speaking, we say that a random vector $\mathbf{X} = (X_1, \dots, X_d)$ follows a *normal variance mixture*, denoted $\mathbf{X} \sim \text{NVM}_d(\boldsymbol{\mu}, \Sigma, F_W)$, if, in distribution,

$$\mathbf{X} = \boldsymbol{\mu} + \sqrt{W} \mathbf{A} \mathbf{Z}, \quad (1)$$

where $\boldsymbol{\mu} \in \mathbb{R}^d$ denotes the *location (vector)*, $\Sigma = \mathbf{A} \mathbf{A}^\top$ for $\mathbf{A} \in \mathbb{R}^{d \times k}$ is the *scale (matrix)* (a covariance matrix), and $W \sim F_W$ is a non-negative random variable independent of $\mathbf{Z} \sim \text{N}_k(\mathbf{0}, I_k)$ (where $I_k \in \mathbb{R}^{k \times k}$ denotes the identity matrix), which we can think of as the mixing variable; see, for example, McNeil et al. (2015, Section 6.2). Note that $(\mathbf{X} | W) \sim \text{N}_d(\boldsymbol{\mu}, W \Sigma)$, hence the name of this class of distributions. This implies that if $\mathbb{E}(\sqrt{W}) < \infty$, then $\mathbb{E}(\mathbf{X}) = \boldsymbol{\mu}$, and if $\mathbb{E}(W) < \infty$, then $\text{cov}(\mathbf{X}) = \mathbb{E}(W) \Sigma$ and $\text{corr}(\mathbf{X}) = P$ (the correlation matrix corresponding to Σ). Furthermore, note that in the latter case with $\mathbf{A} = I_d$ (so when the components of \mathbf{X} are uncorrelated) the components of \mathbf{X} are independent if and only if W is constant almost surely and thus \mathbf{X} is multivariate normal; see McNeil et al. (2015, Lemma 6.5). The multivariate t distribution is obtained by letting W have an inverse-gamma distribution. In what follows we focus on the case $k = d$ in which \mathbf{A} is typically the Cholesky factor computed from a given Σ ; other decompositions of Σ into $\mathbf{A} \mathbf{A}^\top$ for some $\mathbf{A} \in \mathbb{R}^{d \times d}$ can be obtained from the eigendecomposition or singular-value decomposition.

Working with normal variance mixtures (as with any other multivariate distribution) often involves four tasks: sampling, computing the joint distribution function, computing the joint density function as well as parameter estimation. Sampling is straightforward via (1) based on the Cholesky factor \mathbf{A} of Σ .

In contrast, evaluating multivariate distribution functions (such as the normal and the t) is a difficult, yet important problem that has gained much attention in the last couple of decades; see, for instance, Genz (1992), Hickernell and Hong (1997), Genz and Bretz (1999), Genz and Bretz (2002), Genz and Bretz (2009) as well as references therein for a discussion of the estimation of multivariate normal and t probabilities and recent work in Botev and L'Écuyer (2015) for the evaluation of truncated multivariate t distributions. To further

1 Introduction

illustrate how challenging this problem is, we note that the R package `mvtnorm` (one of the most widely used packages according to reverse depends, see Eddelbuettel (2012)) and other R packages do not even provide functionality for evaluating the distribution function of the well-known multivariate t distribution for non-integer degrees of freedom $\nu > 0$.

In this paper, we propose efficient algorithms for computing the joint distribution function and joint density function of a normal variance mixture, and also for estimating its parameters. The only requirement we have for the normal variance mixture is that we must have access to a (possibly numerical) procedure to evaluate the quantile function of W . The assumption that such “black-box” procedure is available to evaluate the quantile is something we refer to as having a *computationally tractable* quantile function for W . Providing algorithms for the above tasks for a more general family of distributions than what currently exists in the literature is one of the main contributions of this work.

The algorithm we propose to efficiently evaluate the joint distribution function of a normal variance mixture (including the case when Σ is singular) is obtained by generalizing methods by A. Genz and F. Bretz to evaluate the distribution function of the multivariate normal and t distribution. In particular, we generalize a variable reordering algorithm originally suggested by Gibson et al. (1994) and adapted by Genz and Bretz (2002) which significantly reduces the variance of the integrand yielding fast convergence of our estimators. We also propose a different approach for using RQMC methods within the integration routine required to evaluate the joint distribution function. Our approach better leverages the improved convergence properties of these methods compared to Monte Carlo sampling. In addition, we explore the synergy between these methods and the variable reordering algorithm using the concept of Sobol’ indices and effective dimension, thus providing new insight on why the reordering algorithm works so well. Sections 3 and 4 respectively include the discussion of RQMC methods and the tasks of evaluating the joint distribution function.

Regarding the joint density function of \mathbf{X} , when going from a simple case such as the multivariate normal to a general normal variance mixture, it can go from being available in closed form to requiring the numerical evaluation of an intractable one-dimensional integral. An example of the latter situation is when W follows an inverse-Burr distribution. Since our goal is to provide algorithms that work for any normal variance mixture, an efficient algorithm to approximate the joint (log)-density function of \mathbf{X} is needed. We tackle this by proposing in Section 5 an adaptive RQMC algorithm that mostly samples in certain important subdomains of the range of the mixing variable to efficiently estimate the log-density of a multivariate normal variance mixture. Even log-densities around -100 can be estimated efficiently.

This flexible algorithm turns out to be a key ingredient for the task of parameter estimation, which we again propose in enough generality to handle any normal variance mixture, as explained in Section 6. More precisely, we employ an ECME (“Expectation/Conditional Maximization Either”) algorithm, which is a likelihood-based fitting procedure developed in Liu and Rubin (1994). This procedure requires repeated evaluations of the log-density function of \mathbf{X} , which is one of the reasons why efficient algorithms for the latter are important when this density does not have a closed form.

2 Normal variance mixture distribution function and density

An extensive numerical study for all proposed algorithms is included in Section 7. This section also includes a detailed investigation of why the reordering algorithm works well with RQMC methods, as well as a data analysis with real-world financial data.

All presented algorithms are available in our R package `nvmmix` (in particular, via `rnvmix()`, `pnvmix()`, `dnvmix()` and `fitnvmix()`; see also `vignette(nvmmix_functionality)`) and the conducted simulations are reproducible with the demo `numerical_experiments`; see Hofert, Hintz, et al. (2020).

To the best of our knowledge, none of the four aforementioned tasks have been discussed in the literature in such generality where the only requirement is to have a computationally tractable quantile function for the mixing variable W . By specifying the latter, methods developed in this paper (and the implementation in `nvmmix`) can be used to perform standard modeling tasks for multivariate normal variance mixtures well beyond the case of a multivariate t distribution. To demonstrate this, a real financial data set is analyzed using an inverse-gamma, a Pareto and an inverse-Burr mixture at the end of Section 7.

2 Normal variance mixture distribution function and density

We assume that Σ has full rank so that the density of $\mathbf{X} \sim \text{NVM}_d(\boldsymbol{\mu}, \Sigma, F_W)$ exists. Denote by $D^2(\mathbf{x}; \boldsymbol{\mu}, \Sigma) = (\mathbf{x} - \boldsymbol{\mu})^\top \Sigma^{-1} (\mathbf{x} - \boldsymbol{\mu})$ the (squared) Mahalanobis distance of $\mathbf{x} \in \mathbb{R}^d$ from $\boldsymbol{\mu}$ with respect to (wrt) Σ . By conditioning on W and substituting $w = F_W^\leftarrow(u)$ (where $F_W^\leftarrow(u) = \inf\{w \in [0, \infty) : F_W(w) \geq u\}$, $u \in (0, 1)$, denotes the quantile function of F_W), the density of \mathbf{X} can then be written as

$$\begin{aligned} f_{\mathbf{X}}(\mathbf{x}) &= \int_0^\infty f_{\mathbf{X}|W}(\mathbf{x} | w) dF_W(w) = \int_0^\infty \frac{1}{\sqrt{(2\pi w)^d |\Sigma|}} \exp\left(-\frac{D^2(\mathbf{x}; \boldsymbol{\mu}, \Sigma)}{2w}\right) dF_W(w) \quad (2) \\ &= \int_0^1 \frac{1}{\sqrt{(2\pi F_W^\leftarrow(u))^d |\Sigma|}} \exp\left(-\frac{D^2(\mathbf{x}; \boldsymbol{\mu}, \Sigma)}{2F_W^\leftarrow(u)}\right) du. \quad (3) \end{aligned}$$

Note that this representation holds for the case when W is absolutely continuous, discrete or of mixed type. In the former case, (2) equals

$$f_{\mathbf{X}}(\mathbf{x}) = \int_0^\infty \frac{1}{\sqrt{(2\pi w)^d |\Sigma|}} \exp\left(-\frac{D^2(\mathbf{x}; \boldsymbol{\mu}, \Sigma)}{2w}\right) f_W(w) dw, \quad (4)$$

where f_W denotes the density of W .

Furthermore, note that $f_{\mathbf{X}}(\mathbf{x})$ is decreasing in the Mahalanobis distance $D^2(\mathbf{x}; \boldsymbol{\mu}, \Sigma)$. Thus

$$f_{\mathbf{X}}(\mathbf{x}) \leq f_{\mathbf{X}}(\boldsymbol{\mu}) = \frac{1}{\sqrt{(2\pi)^d |\Sigma|}} \mathbb{E}\left(\frac{1}{W^{d/2}}\right); \quad \mathbf{x} \in \mathbb{R}^d$$

so that $f_{\mathbf{X}}(\mathbf{x})$ is bounded if and only if $\mathbb{E}(W^{-d/2}) < \infty$.

3 Monte Carlo and (randomized) quasi-Monte Carlo methods

Let $F_{\mathbf{X}}(\mathbf{a}, \mathbf{b})$ denote the probability that \mathbf{X} falls into the hyperrectangle spanned by the lower-left endpoint \mathbf{a} and upper-right endpoint \mathbf{b} , where $\mathbf{a}, \mathbf{b} \in \bar{\mathbb{R}}^d$ for $\bar{\mathbb{R}} = \mathbb{R} \cup \{-\infty, \infty\}$ and $\mathbf{a} < \mathbf{b}$ (interpreted componentwise), where we interpret non-finite components as the corresponding limits. Note that the joint distribution function of \mathbf{X} is a special case of $F_{\mathbf{X}}(\mathbf{a}, \mathbf{b})$ since $F_{\mathbf{X}}(\mathbf{x}) := \mathbb{P}(\mathbf{X} \leq \mathbf{x}) = F_{\mathbf{X}}(\mathbf{a}, \mathbf{x})$ for $\mathbf{a} = (-\infty, \dots, -\infty)$. In what follows we write $F(\mathbf{a}, \mathbf{b})$ instead of $F_{\mathbf{X}}(\mathbf{a}, \mathbf{b})$ to simplify notation. For computing $F(\mathbf{a}, \mathbf{b})$ assume (potentially after adjusting \mathbf{a}, \mathbf{b}) that $\boldsymbol{\mu} = \mathbf{0}$ and that Σ has full rank (the singular case will be discussed in Section A). By conditioning and the substitution $w = F_W^{\leftarrow}(u)$ we obtain that

$$\begin{aligned} F_{\mathbf{X}}(\mathbf{a}, \mathbf{b}) &= \mathbb{P}(\mathbf{a} < \mathbf{X} \leq \mathbf{b}) = \mathbb{P}(\mathbf{a} < \sqrt{W} \mathbf{A} \mathbf{Z} \leq \mathbf{b}) = \mathbb{E} \left(\mathbb{P}(\mathbf{a}/\sqrt{W} < \mathbf{A} \mathbf{Z} \leq \mathbf{b}/\sqrt{W} \mid W) \right) \\ &= \mathbb{E} \left(\Phi_{\Sigma}(\mathbf{a}/\sqrt{W}, \mathbf{b}/\sqrt{W}) \right) = \int_0^{\infty} \Phi_{\Sigma}(\mathbf{a}/\sqrt{w}, \mathbf{b}/\sqrt{w}) \, dF_W(w) \\ &= \int_0^1 \Phi_{\Sigma} \left(\mathbf{a}/\sqrt{F_W^{\leftarrow}(u)}, \mathbf{b}/\sqrt{F_W^{\leftarrow}(u)} \right) \, du, \end{aligned} \quad (5)$$

where $\Phi_{\Sigma}(\mathbf{a}, \mathbf{b}) = \mathbb{P}(\mathbf{a} < \mathbf{Y} \leq \mathbf{b})$ for $\mathbf{Y} \sim N_d(\mathbf{0}, \Sigma)$.

3 Monte Carlo and (randomized) quasi-Monte Carlo methods

Quantities of interest in this paper, such as the distribution function of a normal variance mixture, are (after a suitable transformation) expressed as intractable integrals over the unit hypercube $(0, 1)^d$ for some $d \in \mathbb{N}$, i.e.,

$$\mu = \int_{(0,1)^d} g(\mathbf{u}) \, d\mathbf{u}, \quad (6)$$

where $g : (0, 1)^d \rightarrow \mathbb{R}$ is integrable. Monte Carlo (MC) methods approximate μ in (6) by the arithmetic average $\hat{\mu}_n^{\text{MC}} = (1/n) \sum_{i=1}^n g(\mathbf{U}_i)$ where $\mathbf{U}_1, \dots, \mathbf{U}_n \stackrel{\text{ind.}}{\sim} U(0, 1)^d$. An asymptotic $(1 - \alpha)$ -confidence interval (CI) can be approximated for sufficiently large n by

$$\left[\hat{\mu}_n^{\text{MC}} - z_{1-\alpha/2} \hat{\sigma}_g / \sqrt{n}, \hat{\mu}_n^{\text{MC}} + z_{1-\alpha/2} \hat{\sigma}_g / \sqrt{n} \right],$$

where $z_{\alpha} = \Phi^{-1}(\alpha)$ and $\hat{\sigma}_g^2 = \widehat{\text{var}}(g(\mathbf{U}) = \sum_{i=1}^n (g(\mathbf{U}_i) - \hat{\mu}_n^{\text{MC}})^2 / (n - 1)$. One can choose n so that the length of this CI does not exceed a pre-determined absolute error tolerance.

Replacing the (pseudo-random) evaluation points $\mathbf{U}_1, \dots, \mathbf{U}_n$ by a deterministic low-discrepancy point set which aims at filling the unit hypercube in a more homogeneous way, say $P_n = \{\mathbf{v}_1, \dots, \mathbf{v}_n\} \subset [0, 1)^d$, leads to a *quasi-Monte Carlo* (QMC) estimator for μ . QMC methods often provide better estimators than classical MC methods, the deterministic nature of the points in P_n however does not allow for simple error estimation via CIs as was done for the MC estimator $\hat{\mu}_n^{\text{MC}}$. To overcome this, one can randomize the point set P_n in a way such that the points in the resulting point set, say \tilde{P}_n , are uniformly distributed over $(0, 1)^d$ without losing the low-discrepancy of the point set overall. This leads to randomized

3 Monte Carlo and (randomized) quasi-Monte Carlo methods

QMC (RQMC) methods. In our algorithms, we use a digitally-shifted Sobol' sequence (Sobol' (1967)) as implemented in the function `sobol()`, `randomize = "digital.shift"` of the R package `qrng`; see Hofert and Lemieux (2019). We remark that generating \tilde{P}_n is slightly faster than generating $U_1, \dots, U_n \stackrel{\text{ind.}}{\sim} U(0, 1)^d$ using R's default (pseudo-)random number generator, the Mersenne Twister.

Given B independently randomized copies of P_n , say $\tilde{P}_{n,b} = \{\mathbf{u}_{1,b}, \dots, \mathbf{u}_{n,b}\}$ for $b = 1, \dots, B$, one can construct B independent RQMC estimators of the form

$$\hat{\mu}_{b,n}^{\text{RQMC}} = \frac{1}{n} \sum_{i=1}^n g(\mathbf{u}_{i,b}), \quad b = 1, \dots, B, \quad (7)$$

and combine them to the RQMC estimator

$$\hat{\mu}_n^{\text{RQMC}} = \frac{1}{B} \sum_{b=1}^B \hat{\mu}_{b,n}^{\text{RQMC}} \quad (8)$$

of μ . An approximate $(1 - \alpha)$ -CI for μ can be estimated as

$$\left[\hat{\mu}_n^{\text{RQMC}} - z_{1-\alpha/2} \hat{\sigma}_{\hat{\mu}_n^{\text{RQMC}}} / \sqrt{B}, \hat{\mu}_n^{\text{RQMC}} + z_{1-\alpha/2} \hat{\sigma}_{\hat{\mu}_n^{\text{RQMC}}} / \sqrt{B} \right], \quad (9)$$

where

$$\hat{\sigma}_{\hat{\mu}_n^{\text{RQMC}}} = \sqrt{\frac{1}{B-1} \sum_{i=1}^B (\hat{\mu}_{b,n}^{\text{RQMC}} - \hat{\mu}_n^{\text{RQMC}})^2}. \quad (10)$$

One can compute $\hat{\mu}_n^{\text{RQMC}}$ from (8) for some initial sample size n (e.g., $n = 2^7$) and iteratively increase the sample size of each $\hat{\mu}_{b,n}^{\text{RQMC}}$ in (7) until the length of the CI in (9) satisfies a pre-specified error tolerance. In our implementations, we use $B = 15$, an absolute default error tolerance $\varepsilon = 0.001$ (which can be changed by the user) and $z_{1-\alpha/2} = 3.5$ (so $\alpha \approx 0.00047$). By using $\hat{\mu}_n^{\text{RQMC}}$ as approximation for the true value of μ , one can also consider relative errors instead of absolute errors.

Function evaluations from iterations that did not meet the tolerance can be recycled as follows. Let $P_{n_1, n_2} = \{\mathbf{v}_{n_1+1}, \dots, \mathbf{v}_{n_1+n_2}\}$ be the point set consisting of the n_2 low-discrepancy points after skipping the first n_1 -many points. Furthermore, let $\tilde{P}_{n_1, n_2, b} = \{\mathbf{u}_{n_1+1,b}, \dots, \mathbf{u}_{n_1+n_2,b}\}$ be the b th randomly shifted version of P_{n_1, n_2} and let

$$\hat{\mu}_{b, n_1, n_2}^{\text{RQMC}} = \frac{1}{n_2} \sum_{\mathbf{u} \in \tilde{P}_{n_1, n_2, b}} g(\mathbf{u}), \quad b = 1, \dots, B.$$

If $\hat{\mu}_{n_1}^{\text{RQMC}}$ does not meet the error tolerance, an estimator based on $n_1 + n_2$ points can be calculated using only n_2 additional function evaluations based on

$$\hat{\mu}_{b, 0, n_2}^{\text{RQMC}} = \frac{n_1 \times \hat{\mu}_{b, 0, n_1}^{\text{RQMC}} + n_2 \times \hat{\mu}_{b, n_1, n_2}^{\text{RQMC}}}{n_1 + n_2}, \quad b = 1, \dots, B.$$

3 Monte Carlo and (randomized) quasi-Monte Carlo methods

In iteration i this update is being done with $n_1 = in_0$ and $n_2 = n_1 + n_0$ in Step 3.1) of our Algorithm 3.1 to estimate μ from (6). That is, we start with initial sample size n_0 and add another n_0 points in each iteration. We highlight that this update can be easily implemented for a Sobol' sequence, as one can generate P_{n_1, n_2} efficiently without having to generate P_{0, n_2} ; in R, this can be achieved by calling `sobol(, skip = n1)`. We do not lose any low-discrepancy properties of the randomized Sobol' sequences as the resulting estimator is mathematically equivalent to $\hat{\mu}_{n^*}^{\text{RQMC}} = (1/B) \sum_{b=1}^B \hat{\mu}_{b, 0, n^*}^{\text{RQMC}}$ where n^* is the total number of function evaluations in each randomization. We therefore leverage convergence properties in n of Sobol' sequence based estimators. It is important to point out that the reason why we can add points in this way without discarding previous function evaluations is because the Sobol' sequence is extensible in n . That is, it is constructed as a sequence in such a way that the first n points can be used as a low-discrepancy point set P_n for any n , with additional uniformity properties when n is a power of 2 (or a multiple of a power of 2).

The update in our algorithm is conceptually different from updates in RQMC methods suggested in our references: For instance, the RQMC algorithm proposed in Genz and Bretz (2002) to estimate the distribution function of a multivariate t distribution, therein referred to as QRSVN algorithm, is based on a randomized Korobov rule (which belong to the wider class of lattice rules; see Keast (1973) and Cranley and Patterson (1976)). The QRSVN algorithm also iteratively evaluates the integrand at low-discrepancy points until the estimated error is small enough; however, it does not move along the same sequence of low-discrepancy points from one iteration to another. In iteration i , their method computes an estimator based on a lattice of size p_i (a prime), and estimators from different iterations are combined as a variance-weighted average. Ultimately, the QRSVN algorithm outputs a weighted average of $B \cdot i^*$ different RQMC estimators based on different sample sizes (where i^* denotes the number of iterations needed until termination), whereas our algorithm outputs the average of B digitally-shifted RQMC estimators based on the first n^* points of a Sobol' sequence. Hence, our methods leverage properties of the Sobol' sequence with growing n rather than combining more and more RQMC estimators of different sample sizes. Our proposed approach is thus superior because the variance of RQMC estimators can be shown to be in $O(n^{-\delta})$ with $\delta > 1$ (and the smoother f is, the larger δ is). Hence for a given fixed computing budget of Bn function evaluations that must be split between B and the size n for the point set P_n , it is best to try to take B just large enough so that we get a reasonable variance estimate, and then set n as large as possible in order to further reduce the variance thanks to its $O(n^{-\delta})$ behavior: this is precisely what our approach does. Numerical results in Section 7.2 illustrate how this leads to improved efficiency compared to the QRSVN algorithm.

Finally, our way of updating merely requires Bn_0 additional function evaluations in each iteration, rather than Bp_{i+1} . This typically leads to a smaller run-time, as only as many function evaluations as needed are computed.

Algorithm 3.1 (RQMC Algorithm to estimate $\mu = \int_{(0,1)^d} g(\mathbf{u}) \, d\mathbf{u}$)

Given ε , B , n_0 , i_{\max} , estimate $\mu = \int_{(0,1)^d} g(\mathbf{u}) \, d\mathbf{u}$ via:

3 Monte Carlo and (randomized) quasi-Monte Carlo methods

- 1) Set $n = n_0$, $i = 1$, and compute $\hat{\mu}_{b,n}^{\text{RQMC}} = \hat{\mu}_{b,0,n_0}^{\text{RQMC}}$ for $b = 1, \dots, B$ and $\hat{\mu}_n^{\text{RQMC}}$ from (7) and (8).
- 2) Set $\hat{\varepsilon} = 3.5\hat{\sigma}_{\hat{\mu}_n^{\text{RQMC}}}$ with $\hat{\sigma}_{\hat{\mu}_n^{\text{RQMC}}}$ from (10).
- 3) While $\hat{\varepsilon} > \varepsilon$ and $i \leq i_{\max}$ do:
 - 3.1) Set $n = n + n_0$, compute $\hat{\mu}_{b,in_0,(i+1)n_0}^{\text{RQMC}}$, $b = 1, \dots, B$ and set $\hat{\mu}_{b,n}^{\text{RQMC}} = (i\hat{\mu}_{b,n}^{\text{RQMC}} + \hat{\mu}_{b,in_0,(i+1)n_0}^{\text{RQMC}})/(i+1)$.
 - 3.2) Update $\hat{\mu}_n^{\text{RQMC}} = (1/B) \sum_{b=1}^B \hat{\mu}_{b,n}^{\text{RQMC}}$ and update $\hat{\varepsilon} = 3.5\hat{\sigma}_{\hat{\mu}_n^{\text{RQMC}}}$ with $\hat{\sigma}_{\hat{\mu}_n^{\text{RQMC}}}$ from (10).
 - 3.3) Set $i = i + 1$.
- 4) Return $\hat{\mu}_n^{\text{RQMC}}$.

Sometimes it is necessary to estimate $\log \mu$ rather than μ ; in particular, when μ is small. For instance, if $\mu = f(\mathbf{x})$ where $f(\mathbf{x})$ is the density function of $\mathbf{X} \sim \text{NVM}_d(\boldsymbol{\mu}, \Sigma, F_W)$ evaluated at $\mathbf{x} \in \mathbb{R}^d$, interest may lie in $\log(\mu) = \log f(\mathbf{x})$ as this quantity is needed to compute the log-likelihood of a random sample (which then may be optimized over some parameter space). When μ is small, using $\log \mu \approx \log(\hat{\mu}_n^{\text{RQMC}})$ directly should be avoided. One should instead compute a numerically more robust estimator for $\log \mu$, a *proper logarithm*. To this end, define the function LSE (for Logarithmic Sum of Exponentials) as

$$\text{LSE}(c_1, \dots, c_n) = \log \left(\sum_{i=1}^n \exp(c_i) \right) = c_{\max} + \log \left(\sum_{i=1}^n \exp(c_i - c_{\max}) \right),$$

where $c_1, \dots, c_n \in \mathbb{R}$ and $c_{\max} = \max\{c_1, \dots, c_n\}$. The right-hand side of this equation is numerically more stable than the left-hand side as the sum inside the logarithm is bounded between 1 and n .

Let $c_{i,b} = \log g(u_{i,b})$ for $i = 1, \dots, n$ and $b = 1, \dots, B$. An estimator numerically superior (but mathematically equivalent) to $\log(\hat{\mu}_n^{\text{RQMC}})$ is given by

$$\hat{\mu}_{n,\log}^{\text{RQMC}} = -\log(B) + \text{LSE}(\hat{\mu}_{1,n,\log}^{\text{RQMC}}, \dots, \hat{\mu}_{B,n,\log}^{\text{RQMC}}), \quad (11)$$

where

$$\hat{\mu}_{b,n,\log}^{\text{RQMC}} = -\log(n) + \text{LSE}(c_{1,b}, \dots, c_{n,b}), \quad b = 1, \dots, B. \quad (12)$$

The standard deviation of $\hat{\mu}_{n,\log}^{\text{RQMC}}$ is estimated in the usual way by computing the sample standard deviation of $\hat{\mu}_{1,n,\log}^{\text{RQMC}}, \dots, \hat{\mu}_{B,n,\log}^{\text{RQMC}}$ so that, as before, the integration error can be estimated from the length of the CI in (9). A summary of the procedure to estimate $\log \mu$ with a proper logarithm via RQMC is given in Algorithm C.1 in the appendix. Note that despite the fact that the problem under study here is a one-dimensional integral, we refer to our algorithm as being in the RQMC family. We do so because although the

distinctive features of RQMC mostly have to do with how they design low-discrepancy point sets in dimension larger than 1, another distinctive feature they have is to make use of low-discrepancy sequences that are extensible in n , which is precisely what we are exploiting for this algorithm.

For more information about RQMC methods and their applications in the financial literature, see, e.g., Niederreiter (1992), Lemieux (2009) and Glasserman (2013).

4 Computing the distribution function

As mentioned in the introduction, throughout this paper we assume that the quantile function F_W^\leftarrow of W is computationally tractable (possibly through an approximation). Assume furthermore that the scale matrix Σ has full rank; the evaluation of singular normal variance mixtures is discussed in A.

One might be tempted to sample $U_i \stackrel{\text{ind.}}{\sim} \text{U}(0, 1)$, $i = 1, \dots, n$, and then approximate the integral in (5) by the conditional Monte Carlo estimator

$$F(\mathbf{a}, \mathbf{b}) \approx \hat{\mu}_F^{\text{CMC}} = \frac{1}{n} \sum_{i=1}^n \Phi_\Sigma \left(\mathbf{a} / \sqrt{F_W^\leftarrow(U_i)}, \mathbf{b} / \sqrt{F_W^\leftarrow(U_i)} \right).$$

However, Φ_Σ itself is a d -dimensional integral typically evaluated by RQMC methods, so this approach would be time-consuming. Hence, the first step should be to approximate Φ_Σ . To this end, we follow Genz (1992) and start by expressing Φ_Σ (and then $F(\mathbf{a}, \mathbf{b})$) as integrals over the unit hypercube. In the second part of this section, we derive an efficient RQMC algorithm to approximate $F(\mathbf{a}, \mathbf{b})$ based on Algorithm 3.1. In particular, it details how a significant variance reduction (and hence decrease in run time) can be achieved through a variable reordering following an approach originally suggested by Gibson et al. (1994) for multivariate normal probabilities and later adapted by Genz and Bretz (2002) to work for multivariate t probabilities.

The novelty of our approach for this problem is three-fold: first, our algorithm applies to any normal variance mixture; second, it uses RQMC methods in a way that better leverages their convergence properties, compared to previous work done for the multivariate normal and t distributions, and third, we include a detailed analysis (with our numerical results, in Section 7.2.2) of why the reordering algorithm works well with RQMC methods.

4.1 Reformulation of the integral

We now address Φ_Σ . Let $C = (C_{ij})_{i,j=1}^d$ be the Cholesky factor of Σ , i.e., a lower triangular matrix satisfying $CC^\top = \Sigma$. Denote by C_k^\top the k th row of C for $k = 1, \dots, d$. Genz (1992) (see also Genz and Bretz (1999), Genz and Bretz (2002) and Genz and Bretz (2009)) uses a series of transformations that rely on the lower triangular structure of C to produce a

4 Computing the distribution function

separation of variables as follows:

$$\begin{aligned}\Phi_{\Sigma}(\mathbf{a}, \mathbf{b}) &= \int_{a_1}^{b_1} \cdots \int_{a_d}^{b_d} \frac{1}{\sqrt{(2\pi)^d |\Sigma|}} \exp\left(-\frac{\mathbf{x}^\top \Sigma^{-1} \mathbf{x}}{2}\right) d\mathbf{x} \\ &= (\hat{e}_1 - \hat{d}_1) \int_0^1 (\hat{e}_2 - \hat{d}_2) \cdots \int_0^1 (\hat{e}_d - \hat{d}_d) du_{d-1} \cdots du_1,\end{aligned}\quad (13)$$

where the \hat{d}_i and \hat{e}_i are recursively defined via

$$\hat{e}_1 = \Phi\left(\frac{b_1}{C_{11}}\right), \hat{e}_i = \hat{e}_i(u_1, \dots, u_{i-1}) = \Phi\left(\frac{b_i - \sum_{j=1}^{i-1} C_{ij} \Phi^{-1}(\hat{d}_j + u_j(\hat{e}_j - \hat{d}_j))}{C_{ii}}\right),$$

and \hat{d}_i is \hat{e}_i with b_i replaced by a_i for $i = 1, \dots, d$. Note that the final integral in (13) is $(d-1)$ -dimensional.

With this at hand, we can write (5) as

$$F(\mathbf{a}, \mathbf{b}) = \int_{(0,1)^d} g(\mathbf{u}) d\mathbf{u} = \int_0^1 g_1(u_0) \int_0^1 g_2(u_0, u_1) \cdots \int_0^1 g_d(u_0, \dots, u_{d-1}) du_{d-1} \cdots du_0, \quad (14)$$

where

$$g(\mathbf{u}) = \prod_{i=1}^d g_i(u_0, \dots, u_{i-1}), \quad g_i(u_0, \dots, u_{i-1}) = e_i - d_i, \quad i = 1, \dots, d, \quad (15)$$

for $\mathbf{u} = (u_0, u_1, \dots, u_{d-1}) \in (0, 1)^d$. The e_i are recursively defined by

$$\begin{aligned}e_1 &= e_1(u_0) = \Phi\left(\frac{b_1}{C_{11} \sqrt{F_W^{\leftarrow}(u_0)}}\right), \\ e_i &= e_i(u_0, \dots, u_{i-1}) = \Phi\left(\frac{1}{C_{ii}} \left(\frac{b_i}{\sqrt{F_W^{\leftarrow}(u_0)}} - \sum_{j=1}^{i-1} C_{ij} \Phi^{-1}(d_j + u_j(e_j - d_j))\right)\right),\end{aligned}\quad (16)$$

for $i = 2, \dots, d$ and the d_i are e_i with b_i replaced by a_i for $i = 1, \dots, d$. We remark that there is a typo (wrong bracket) in the corresponding formula for the special case of a multivariate t distribution in Genz and Bretz (2002, p. 958).

Summarizing, the original $(d+1)$ dimensional integral is reduced to

$$F(\mathbf{a}, \mathbf{b}) = \int_{(0,1)^d} g(\mathbf{u}) d\mathbf{u},$$

with the function g defined in (15) so that RQMC methods from Section 3 could be applied directly to the problem in this form to estimate $F(\mathbf{a}, \mathbf{b})$. As pointed out in Genz and Bretz (2009), the transformations undertaken in this section to produce a separation of variables essentially describe a Rosenblatt transform; see Rosenblatt (1952).

4.2 Variable reordering and RQMC estimation

Inspecting (14) and (16), we see that the sampled component u_j of \mathbf{u} in the j th integral affects the ranges of all g_k with $k > j$. Observe that permuting the order in \mathbf{a} , \mathbf{b} and Σ does not affect the value of $F(\mathbf{a}, \mathbf{b})$ as long as the same permutation is applied to \mathbf{a} , \mathbf{b} and to both the rows and columns of Σ . It therefore seems to be a fruitful approach to choose a permutation of \mathbf{a} , \mathbf{b} and Σ such that g_2 has, on average, the smallest range; g_3 the second smallest, and so on. This has been observed in Gibson et al. (1994) in the context of calculating multivariate normal probabilities and has been adapted by Genz and Bretz (2002) to handle multivariate t integrals. As in the latter reference, one can sort the integration limits a priori according to their expected length of integration limits. This is more complicated than just ordering \mathbf{a} , \mathbf{b} and Σ according to the lengths $b_i - a_i$ (assuming all of them are finite) as the latter does not take into account the dependence of the components in \mathbf{X} . We generalize the Gibson, Glasbey and Elston method for reordering according to expected ranges to work for normal variance mixture distribution functions in Algorithm C.2 in the appendix.

From a simulation point of view, the particular value of u_1 will affect the ranges of all the remaining $d - 2$ integrals. Indeed, each input $\mathbf{u} = (u_0, \dots, u_{d-1}) \sim \text{U}(0, 1)^d$ is transformed to a product of conditional probabilities: The first component, u_0 , is used to sample from the mixing variable via inversion; $g_1(u_0)$ is then the conditional probability of the first component of the random vector \mathbf{X} falling into (a_1, b_1) given that $W = F_W^{\leftarrow}(u_0)$, that is $g_1(u_0) = \mathbb{P}(X_1 \in (a_1, b_1) \mid W = F_W^{\leftarrow}(u_0))$. Next, u_1 is transformed to $y_1 = \Phi^{-1}(d_1 + u_1(e_1 - d_1))$, which is a realization of the random variable $(X_1 \mid X_1 \in (a_1, b_1), W = F_W^{\leftarrow}(u_0))$. Then, $g_2(u_0, u_1) = \mathbb{P}(X_2 \in (a_2, b_2) \mid X_1 = y_1, W = F_W^{\leftarrow}(u_0))$ and so on and so forth. As we are conditioning on events of the form $\{X_1 = y_1, \dots, X_l = y_l, W = F_W^{\leftarrow}(u_0)\}$ for all subsequent probabilities, this also explains why variable reordering can help decrease the variance: It is designed in a way so that X_1 has smallest (expected) range, X_2 second smallest and so on. In the explanation above, if $b_1 - a_1$ is small, there is only little variability in y_1 so that $g(u_0, u_1)$ should be close to $\mathbb{P}(X_2 \in (a_2, b_2) \mid X_1 \in (a_1, b_1), W = F_W^{\leftarrow}(u_0))$. We point out that if $F_W^{\leftarrow}(u)$ is a non-zero constant for all $u \in (0, 1)$ (corresponding to \mathbf{X} being multivariate normal), this is the original derivation in Gibson et al. (1994) who independently developed a Monte Carlo procedure to approximate multivariate normal probabilities similar to Genz (1992).

Algorithm C.2 is a greedy procedure that only reorders \mathbf{a} , \mathbf{b} , Σ (and updates the Cholesky factor C accordingly). Changing the order in \mathbf{a} , \mathbf{b} and Σ does not introduce any bias so that one can use a rather crude approximation for $\mu_{\sqrt{W}}$ for $\mathbb{E}(\sqrt{W})$ if the true mean is not known. Note also that variable reordering needs to be performed only once before applying RQMC to the integrand g in (15) so that the cost of reordering is low compared to the overall cost of evaluating $F(\mathbf{a}, \mathbf{b})$.

Our method to estimate $F(\mathbf{a}, \mathbf{b})$ is summarized in Algorithm 4.1.

Algorithm 4.1

Given $\mathbf{a}, \mathbf{b}, \Sigma, \varepsilon, B, n_0, i_{\max}$, estimate $F(\mathbf{a}, \mathbf{b})$ as follows:

5 Computing the (logarithmic) density

- 1) Apply the reordering Algorithm C.2 to the inputs $\mathbf{a}, \mathbf{b}, \Sigma$.
- 2) Apply Algorithm 3.1 on the integrand $(g(\mathbf{u}) + g(\mathbf{1} - \mathbf{u}))/2$ with g from (15) and reordered inputs.

In Section 7.2 it is shown through a simulation study that this (rather cheap) variable reordering can yield a great variance reduction for the RQMC algorithm, Algorithm 4.1. A detailed study as to why this works so well is included in Section 7.2.2.

Note that parallelization of our methods, i.e., estimation of $F(\mathbf{a}_i, \mathbf{b}_i)$, $i = 1, \dots, n$, simultaneously is difficult for two reasons: Reordering needs to be performed for each input $\mathbf{a}_i, \mathbf{b}_i$ separately so that Algorithm C.2 needs to be called n times. Furthermore, the structure of the integrand g from (15) (see also (16)) does not allow for an efficient implementation of common random numbers as all quantile evaluations $\Phi^{-1}(\cdot)$ depend on the limits \mathbf{a}, \mathbf{b} so that they cannot be recycled.

5 Computing the (logarithmic) density

We now turn to the task of computing the (logarithmic) density function of a normal variance mixture. Let us first point out that the main reason why we need to be able to evaluate the density function is for the fitting procedure, which is likelihood-based and is explained in detail in Section 6. Now, since our goal is to be able to cover all normal variance mixtures, we cannot assume that the density function of \mathbf{X} is available in closed form. Indeed, a closed form for $f_{\mathbf{X}}(\mathbf{x})$ exists in some cases (e.g., when W is an inverse-gamma or Pareto), but not in all cases (e.g., when W follows an inverse-Burr distribution, a model actually used with success in Section 7.2). For those latter cases, an efficient approximation is needed, as there is likely to be a repeated need for evaluating the density (or log-density) within the fitting procedure. This also means that fitting algorithms proposed for the multivariate t cannot be directly adapted for the general normal variance mixture case, as they would not include functionalities able to deal with a density that does not exist in closed form. Below we propose an adaptive RQMC algorithm to deal with those cases, which is based on the ideas presented in Section 3.

From (3) it follows that computing the density requires the evaluation of the univariate integral $\mu := f_{\mathbf{X}}(\mathbf{x}) = \int_0^1 h(u) du$, where

$$h(u) = \frac{1}{\sqrt{(2\pi F_W^{\leftarrow}(u))^d |\Sigma|}} \exp\left(-\frac{D^2(\mathbf{x}; \boldsymbol{\mu}, \Sigma)}{2F_W^{\leftarrow}(u)}\right), \quad u \in (0, 1). \quad (17)$$

To simplify notation, we write $f(\mathbf{x})$ instead of $f_{\mathbf{X}}(\mathbf{x})$ whenever confusion is not possible.

For likelihood-based methods one should compute the logarithmic density (or *log-density*) rather than the density. Since $f(\mathbf{x})$ is expressed as a univariate integral over $(0, 1)$, Algorithm C.1, that is, RQMC methods combined with a proper logarithm as described at the end of Section 3 on Page 8, can be applied directly to estimate $\log(\mu) = \log f(\mathbf{x})$ via RQMC. In fact, given inputs $\mathbf{x}_1, \dots, \mathbf{x}_N$, the log-densities $\log f(\mathbf{x}_1), \dots, \log f(\mathbf{x}_N)$ can be

5 Computing the (logarithmic) density

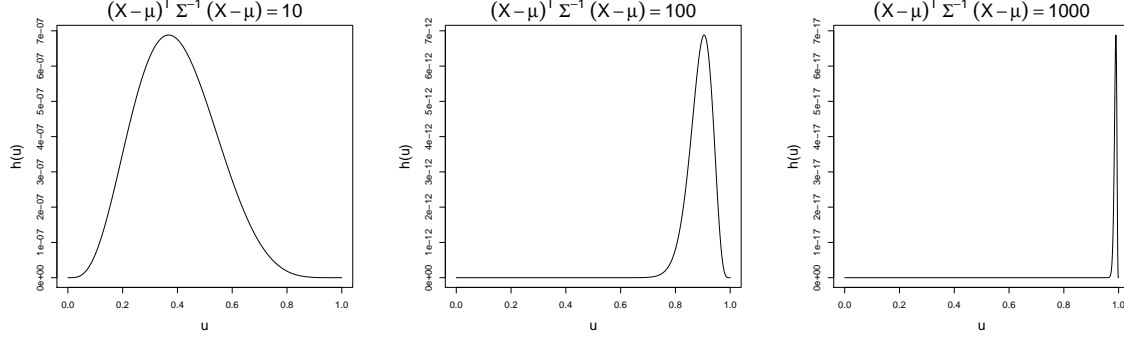


Figure 1 Integrand h for a 10-dimensional t distribution with 2 degrees of freedom.

estimated simultaneously by using the same realizations of W , i.e., using the same $F_W^{\leftarrow}(u_{i,b})$ for all inputs \mathbf{x}_k , $k = 1, \dots, N$, until the precision is reached for all inputs. This procedure, i.e. estimating $\log \mu$ directly based on (17) via RQMC, will be referred to as the *crude procedure*.

It turns out that the crude procedure works sufficiently well for inputs \mathbf{x} with small to moderate Mahalanobis distances, but deteriorates for larger Mahalanobis distances. The reason is that the overall shape of the integrand h is heavily influenced by $D^2(\mathbf{x}; \boldsymbol{\mu}, \Sigma)$ and for large values, most of the mass is concentrated in a small domain of $(0, 1)$. This is illustrated in Figure 1 where the integrand $h(u)$ is plotted against u in the special case where \mathbf{X} follows a multivariate t distribution in dimension 10 with 2 degrees of freedom. For instance, in the right-most plot, most of the mass is concentrated near 1. It thus seems to be a fruitful approach to tailor the integration routine in a way so that it samples mostly in this relevant domain around the maximum, giving rise to an *adaptive algorithm*. To this end, we summarize some properties of the function h in the following lemma which can be shown using elementary calculus.

Lemma 5.1

Let W have a continuous distribution supported on the whole positive real line. Then, the function h from Equation (17) is continuous on $(0, 1)$, satisfies $h(0) = h(1) = 0$ and $h(u) > 0$ for $u \in (0, 1)$. Furthermore, the maximum value of h on $(0, 1)$, i.e., $h_{\max} = \max\{h(u) : u \in [0, 1]\}$ is attained in the interior of $(0, 1)$. The maximum is attained at

$$u^* = F_W \left(\frac{D^2(\mathbf{x}; \boldsymbol{\mu}, \Sigma)}{d} \right) \text{ with } h(u^*) = \left(\frac{2\pi|\Sigma|^{1/d} \cdot D^2(\mathbf{x}; \boldsymbol{\mu}, \Sigma)}{d} \right)^{-d/2} \exp \left(-\frac{d}{2} \right) \quad (18)$$

so that h_{\max} is independent of the distribution of W . Finally, h is strictly increasing on $(0, u^*)$ and strictly decreasing on $(u^*, 1)$.

Equation (18) is crucial for the adaptive algorithm we propose: The value h_{\max} , i.e., the height of the peak of the integrand h , is independent of the distribution of W as long as

5 Computing the (logarithmic) density

W is continuous and supported on the whole positive real line. If W is continuous but has bounded support, h_{\max} may need to be replaced by $h(0)$ or $h(1)$. If W is discrete, the problem becomes trivial as an analytical formula for the density is available in this case.

The idea is now to apply RQMC to a relevant region around u^* from (18), which can be done as follows: Given a threshold ε_{th} with $0 < \varepsilon_{\text{th}} \ll h_{\max}$, the structure of the integrand h guarantees the existence of u_l and u_r (l for “left” and r for “right”) with $0 < u_l < u^* < u_r < 1$ so that $h(u) > \varepsilon_{\text{th}}$ if and only if $u \in (u_l, u_r)$. For instance, take

$$\varepsilon_{\text{th}} = 10^{\log(h_{\max})/\log(10) - k_{\text{th}}} \quad (19)$$

with $k_{\text{th}} = 10$ so that ε_{th} is 10 orders smaller than h_{\max} . RQMC can then be used in the region (u_l, u_r) by replacing every number $v \in (0, 1)$ by $v' = u_l + (u_r - u_l)v \in (u_l, u_r)$ yielding an estimate for $\log \int_{u_l}^{u_r} h(u) du$. For the remaining regions $(0, u_l)$ and $(u_r, 1)$ we suggest using a crude trapezoidal rule: If $\varepsilon_{\text{th}} \ll h_{\max}$ those regions do not significantly contribute to the overall integral anyway, so a rather cheap and quick procedure is recommended here.

It remains to discuss how the numbers u_l, u^*, u_r can be computed. Recall that the only information available about W is its quantile function F_W^{\leftarrow} in form of a “black box” so that u^* from (18) cannot be computed directly. We suggest using a bisection algorithm to solve the equivalent equation $F_W^{\leftarrow}(u) = \mathbf{x}^\top \Sigma^{-1} \mathbf{x} / d$. Starting values can be found using a small number of pilot runs. Similarly, there is no direct formula for u_l and u_r . While those can be expressed using Lambert’s W function, the lack of information about W does not allow a direct computation. A bisection can be used here as well. Clearly, all pilot runs and all quantile evaluations performed in the bisections should be stored so that those expensive evaluations can be re-used.

It is clear from Figure 1 that the shape of the integrand heavily depends on \mathbf{x} through its Mahalanobis distance, and this holds true for u_l, u^*, u_r as well. As such, the adaptive procedure just described does not allow for simultaneous estimation of $\log f(\mathbf{x}_1), \dots, \log f(\mathbf{x}_N)$ directly, as the regions to which RQMC is applied differ from one input to another one. In order to reduce run time, we suggest using the crude procedure on all inputs $\mathbf{x}_1, \dots, \mathbf{x}_N$ with a small number of iterations (say, $i_{\max} = 4$) first and use the adaptive procedure only for those inputs \mathbf{x}_j whose error estimates did not reach the tolerance. The advantage is that only little run time is spent on estimating “easy” integrals. Furthermore, if $i_{\max} = 4$, $B = 15$ and the initial sample size is $n_0 = 128$, such pilot run gives 7680 pairs $(u, F_W^{\leftarrow}(u))$. These can be used to determine starting values for the bisections to find u_l, u_r and u^* and they can also be used to estimate the integral in the regions $(0, u_l)$ and $(u_r, 1)$ using a trapezoidal rules with non-equidistant knots. The following algorithm summarizes our procedure, which is implemented in the R function `dnvmix(, log = TRUE)` of the R package `nvmix`.

Algorithm 5.2 (Adaptive RQMC Algorithm to estimate $\log f(\mathbf{x}_1), \dots, \log f(\mathbf{x}_N)$)

Given $\mathbf{x}_1, \dots, \mathbf{x}_N$, Σ , ε , $\varepsilon_{\text{bisec}}$, B , i_{\max} , k_{th} , estimate $\log f(\mathbf{x}_l)$, $l = 1, \dots, N$, via:

- 1) Apply Algorithm C.1 with at most i_{\max} iterations on all inputs \mathbf{x}_l , $l = 1, \dots, N$. Store all uniforms and corresponding quantiles $F_W^{\leftarrow}(\cdot)$ in a list, say \mathcal{L} .

5 Computing the (logarithmic) density

- 2) If all estimates $\mu_{\log f(\mathbf{x}_l)}^{\text{RQMC}}$, $l = 1, \dots, N$ meet the error tolerance ε , go to Step 4).
If not, we can assume wlog (after reordering) that \mathbf{x}_s , $s = 1, \dots, N'$ with $1 \leq N' \leq N$ are the inputs whose error estimates did not meet the error tolerance.
- 3) For each remaining input \mathbf{x}_s , $s = 1, \dots, N'$, do the following:
 - 3.1) Determine h_{\max} using (18) and ε_{th} using (19).
 - 3.2) Find maximal $u^{*,l}$ and minimal $u^{*,r}$ in the list \mathcal{L} so that $F_W^{\leftarrow}(u^{*,l}) \leq \mathbf{x}_s^\top \Sigma^{-1} \mathbf{x}_s / d \leq F_W^{\leftarrow}(u^{*,r})$ (which implies $u^{*,l} \leq u^* \leq u^{*,r}$). Use a bisection algorithm with starting values $u^{*,l}$ and $u^{*,r}$ and a tolerance of $\varepsilon_{\text{bisec}}$ to find u^* . Add any additional u 's and $F_W^{\leftarrow}(u)$'s computed in the bisection to the list \mathcal{L} .
 - 3.3) Find the largest number $u_l^{(1)} \in \mathcal{L}$ and the smallest number $u_l^{(2)} \in \mathcal{L}$ such that $u_l^{(1)} \leq u_l^{(2)} \leq u^*$, $h(u_l^{(1)}) \leq \varepsilon_{\text{th}}$ and $h(u_l^{(2)}) \geq \varepsilon_{\text{th}}$. Then $u_l^{(1)} \leq u_l \leq u_l^{(2)} \leq u^*$.
Similarly, find the largest number $u_r^{(1)} \in \mathcal{L}$ and the smallest number $u_r^{(2)} \in \mathcal{L}$ such that $u^* \leq u_r^{(1)} \leq u_r^{(2)}$, $h(u_r^{(1)}) \geq \varepsilon_{\text{th}}$ and $h(u_r^{(2)}) \leq \varepsilon_{\text{th}}$. Then $u^* \leq u_r^{(1)} \leq u_r \leq u_r^{(2)}$.
Then use a bisection to find u_l (using starting values $u_l^{(1)}$ and $u_l^{(2)}$) and u_r (using starting values $u_r^{(1)}$ and $u_r^{(2)}$) with a tolerance of $\varepsilon_{\text{bisec}}$. Add any additional u 's and $F_W^{\leftarrow}(u)$'s computed in the bisection to the list \mathcal{L} .
 - 3.4) Approximate $\log \int_0^{u_l} h(u) du$ using a trapezoidal rule with knots u'_1, \dots, u'_m where u'_i are those u 's in \mathcal{L} satisfying $u \leq u_l$. Call the approximation $\hat{\mu}_{(0,u_l)}(\mathbf{x}_s)$.
 - 3.5) Approximate $\log \int_{u_r}^1 h(u) du$ using a trapezoidal rule with knots u''_1, \dots, u''_p where u''_i are those u 's in \mathcal{L} satisfying $u \geq u_r$. Call the approximation $\hat{\mu}_{(u_r,1)}(\mathbf{x}_s)$.
 - 3.6) Apply Algorithm C.1 where all uniforms $v \in (0, 1)$ are replaced by $v' = u_l + (u_r - u_l)v \in (u_l, u_r)$. Call the output $\log \hat{\mu}$. Then set $\log \hat{\mu}_{(u_l, u_r)} = \log(u_r - u_l) + \log \hat{\mu}$ which estimates $\log \int_{u_l}^{u_r} h(u) du$.
 - 3.7) Combine

$$\hat{\mu}_{\log f(\mathbf{x}_s)}^{\text{RQMC}} = \text{LSE} \left(\hat{\mu}_{(0,u_l)}(\mathbf{x}_s), \hat{\mu}_{(u_l, u_r)}(\mathbf{x}_s), \hat{\mu}_{(u_r, 1)}(\mathbf{x}_s) \right)$$
- 4) Return $\hat{\mu}_{\log f(\mathbf{x}_l)}^{\text{RQMC}}$, $l = 1, \dots, N$

Remark 5.3

Algorithm 5.2 can be applied to estimate a slightly larger class of integrals. Let

$$\mu = \int_0^\infty c w^{-k} \exp(m/w) dF_W(w) = \int_0^\infty \tilde{h}(u) du;$$

here, $k, m > 0$ are constant and $\tilde{h}(u) = c F_W^{\leftarrow}(u)^{-k} \exp(m/F_W^{\leftarrow}(u))$ for $u \in (0, 1)$. A result similar to Lemma 5.1 applies to \tilde{h} (replace d by k in the formula for u^* in (18)). Thus, after only slight adjustments to Algorithm 5.2, the latter can be used to estimate $\log(\mu)$ efficiently. This will be useful in Section 6.

6 Fitting multivariate normal variance mixtures

In this section, we derive an expectation-maximization (EM)-like algorithm whose distinctive feature is that it can estimate the parameters of any given normal variance mixture. Its design is inspired by the ECME algorithm used for fitting multivariate t models, but is appropriately modified to allow for a general mixing variable W . This requirement means that our approach must be able to handle the case where the density $f_{\mathbf{X}}(\mathbf{x})$ may not exist in closed form, and must therefore be approximated. The fact that ECME-type algorithms break the optimization part into two steps—and thus handle the parameters $\boldsymbol{\nu}$ of W 's distribution separately from $\boldsymbol{\mu}$ and Σ —meshes very well with our assumption that all we may know about W is through access to a “black-box” function for its quantile function. That is, since the step to find $\boldsymbol{\nu}$ is done separately, we can easily make it adaptable to whether or not W 's distribution is such that $f_{\mathbf{X}}(\mathbf{x})$ exists in closed form. More precisely, in our R implementation, we assume the user either provides a “black-box” function for the quantile function of W —in which case $f_{\mathbf{X}}(\mathbf{x})$ is approximated using the algorithm described in the previous section—or specifies that W is constant, inverse-gamma, or Pareto, in which case $f_{\mathbf{X}}(\mathbf{x})$ is evaluated exactly. Examples provided in Section 7.2 demonstrate that the versatility of our algorithm, which we now explain, does not come at the cost of decreased accuracy.

Assume $\mathbf{X}_1, \dots, \mathbf{X}_n \stackrel{\text{ind.}}{\sim} \text{NVM}_d(\boldsymbol{\mu}, \Sigma, F_W)$ with unknown location vector $\boldsymbol{\mu}$ and unknown scale matrix Σ where F_W has quantile function $F_W^{\leftarrow}(u; \boldsymbol{\nu})$ with unknown parameter vector $\boldsymbol{\nu}$ of length $p_{\boldsymbol{\nu}}$. For notational convenience, let $\boldsymbol{\theta} = (\boldsymbol{\nu}, \boldsymbol{\mu}, \Sigma^{-1})$ and denote by $\boldsymbol{\theta}_k$ the current value of $\boldsymbol{\theta}$ in iteration k .

Before deriving our algorithm, we need some notation. The original log-likelihood is given by

$$\log L^{\text{org}}(\boldsymbol{\nu}, \boldsymbol{\mu}, \Sigma; \mathbf{X}_1, \dots, \mathbf{X}_n) = \sum_{i=1}^n \log f_{\mathbf{X}}(\mathbf{X}_i; \boldsymbol{\nu}, \boldsymbol{\mu}, \Sigma)$$

and the complete log-likelihood $\log L^c$ can be written as

$$\begin{aligned} \log L^c(\boldsymbol{\theta}; \mathbf{X}_1, \dots, \mathbf{X}_n, W_1, \dots, W_n) &= \sum_{i=1}^n \log f_{\mathbf{X}, W}(\mathbf{X}_i, W_i; \boldsymbol{\theta}) \\ &= \sum_{i=1}^n \log f_{\mathbf{X}|W}(\mathbf{X}_i | W_i; \boldsymbol{\mu}, \Sigma) + \sum_{i=1}^n \log f_W(W_i; \boldsymbol{\nu}), \end{aligned} \tag{20}$$

where W_1, \dots, W_n are (unobserved) iid copies of W . Note that the first sum contains the log-likelihood contributions of $\text{N}_d(\boldsymbol{\mu}, W_i \Sigma)$ and thus is almost the log-likelihood of a normal distribution apart from potentially different W_i (expected, for example, if W is continuously distributed on the whole positive real line). The expected value of the complete log-likelihood given the (observed) data $\mathbf{X}_1, \dots, \mathbf{X}_n$ and current estimate $\boldsymbol{\theta}_k$ is then

$$Q(\boldsymbol{\theta}; \boldsymbol{\theta}_k) = \mathbb{E}(\log L^c(\boldsymbol{\theta}; \mathbf{X}_1, \dots, \mathbf{X}_n, W_1, \dots, W_n) | \mathbf{X}_1, \dots, \mathbf{X}_n; \boldsymbol{\theta}_k). \tag{21}$$

As mentioned earlier, rather than trying to maximize $Q(\boldsymbol{\theta}; \boldsymbol{\theta}_k)$ over $\boldsymbol{\theta}$ as a classical EM algorithm would do, we instead employ an ECME algorithm as developed in Liu and Rubin (1994); see also references therein for more details on variations of the EM algorithm. In this way, and as explained below, optimization is broken into two steps, which respectively deal with $(\boldsymbol{\mu}, \Sigma)$ and $\boldsymbol{\nu}$.

The basic structure of our algorithm is as follows:

Algorithm 6.1 (ECME Algorithm for fitting normal variance mixtures: Main idea)

Given iid data $\mathbf{X}_1, \dots, \mathbf{X}_n$, estimate $\boldsymbol{\mu}, \Sigma, \boldsymbol{\nu}$ via:

- 1) Obtain an initial estimate $\boldsymbol{\theta}_0 = (\boldsymbol{\nu}_0, \boldsymbol{\mu}_0, \Sigma_0^{-1})$
- 2) For $k = 1, \dots$, repeat until convergence
 - 2.1) Update $\boldsymbol{\mu}_k$ and Σ_k by maximizing $Q(\boldsymbol{\theta}; \boldsymbol{\theta}_k)$ with respect to $\boldsymbol{\mu}$ and Σ with $\boldsymbol{\nu} = \boldsymbol{\nu}_{k-1}$ held fixed.
 - 2.2) Update $\boldsymbol{\nu}_k$ by maximizing $\log L^{\text{org}}(\boldsymbol{\nu}, \boldsymbol{\mu}_k, \Sigma_k; \mathbf{X}_1, \dots, \mathbf{X}_n)$ with respect to $\boldsymbol{\nu}$.

That is, in the k 'th iteration, we first update $\boldsymbol{\mu}$ and Σ by maximizing the expected complete log-likelihood conditional on the observed data and then update $\boldsymbol{\nu}$ by maximizing the original likelihood with respect to $\boldsymbol{\nu}$ with $\boldsymbol{\mu}$ and Σ set to their current estimates. This is an ECME algorithm as we either maximize the expected complete log-likelihood or the original likelihood; see also Liu and Rubin (1995) for a discussion of an ECME algorithm for the multivariate t distribution.

Let

$$\xi_{ki} = \mathbb{E}(\log W_i | \mathbf{X}_i; \boldsymbol{\theta}_k) \quad \text{and} \quad \delta_{ki} = \mathbb{E}(1/W_i | \mathbf{X}_i; \boldsymbol{\theta}_k), \quad i = 1, \dots, n.$$

We calculate $Q(\boldsymbol{\theta}; \boldsymbol{\theta}_k)$ from (21) in the following lemma:

Lemma 6.2

$Q(\boldsymbol{\theta}; \boldsymbol{\theta}_k)$ from (21) allows for the decomposition $Q(\boldsymbol{\theta}; \boldsymbol{\theta}_k) = Q_{\mathbf{X}|W}(\boldsymbol{\mu}, \Sigma^{-1}; \boldsymbol{\theta}_k) + Q_W(\boldsymbol{\nu}; \boldsymbol{\theta}_k)$ where

$$Q_{\mathbf{X}|W}(\boldsymbol{\mu}, \Sigma^{-1}; \boldsymbol{\theta}_k) = -\frac{1}{2} \left(nd \log(2\pi) - n \log(\det(\Sigma^{-1})) + \sum_{i=1}^n (D^2(\mathbf{X}_i; \boldsymbol{\mu}, \Sigma) \delta_{ki} + d \xi_{ki}) \right),$$

$$Q_W(\boldsymbol{\nu}; \boldsymbol{\theta}_k) = \sum_{i=1}^n \mathbb{E}(\log f_W(W_i; \boldsymbol{\nu}) | \mathbf{X}_i; \boldsymbol{\theta}_k).$$

Proof. Starting from (21) and using (20) we obtain

$$\begin{aligned} Q(\boldsymbol{\theta}; \boldsymbol{\theta}_k) &= \mathbb{E}(\log L^c(\boldsymbol{\theta}; \mathbf{X}_1, \dots, \mathbf{X}_n, W_1, \dots, W_n) | \mathbf{X}_1, \dots, \mathbf{X}_n; \boldsymbol{\theta}_k) \\ &= \sum_{i=1}^n \mathbb{E}(\log f_{\mathbf{X}|W}(\mathbf{X}_i | W_i; \boldsymbol{\mu}, \Sigma) | \mathbf{X}_1, \dots, \mathbf{X}_n; \boldsymbol{\theta}_k) \\ &\quad + \sum_{i=1}^n \mathbb{E}(\log f_W(W_i; \boldsymbol{\nu}) | \mathbf{X}_1, \dots, \mathbf{X}_n; \boldsymbol{\theta}_k) \end{aligned}$$

6 Fitting multivariate normal variance mixtures

$$\begin{aligned}
&= \sum_{i=1}^n \mathbb{E}(\log f_{\mathbf{X}|W}(\mathbf{X}_i | W_i; \boldsymbol{\mu}, \Sigma) | \mathbf{X}_i; \boldsymbol{\theta}_k) + \sum_{i=1}^n \mathbb{E}(\log f_W(W_i; \boldsymbol{\nu}) | \mathbf{X}_i; \boldsymbol{\theta}_k) \\
&= Q_{\mathbf{X}|W}(\boldsymbol{\mu}, \Sigma^{-1}; \boldsymbol{\theta}_k) + Q_W(\boldsymbol{\nu}; \boldsymbol{\theta}_k)
\end{aligned}$$

where the first expectation is taken with respect to W_1, \dots, W_n for given $\mathbf{X}_1, \dots, \mathbf{X}_n$ and $\boldsymbol{\theta}_k$, and the last line of the displayed equation is understood as the definition of $Q_{\mathbf{X}|W}$ and Q_W . Using that $\mathbf{X} | W \sim N_d(\boldsymbol{\mu}, W\Sigma)$, it is easily verified that

$$\begin{aligned}
Q_{\mathbf{X}|W}(\boldsymbol{\mu}, \Sigma^{-1}; \boldsymbol{\theta}_k) &= \sum_{i=1}^n \mathbb{E}(\log f_{\mathbf{X}|W}(\mathbf{X}_i | W_i; \boldsymbol{\mu}, \Sigma) | \mathbf{X}_i; \boldsymbol{\theta}_k) \\
&= -\frac{1}{2} \left(nd \log(2\pi) - n \log(\det(\Sigma^{-1})) + \sum_{i=1}^n (D^2(\mathbf{X}_i; \boldsymbol{\mu}, \Sigma) \delta_{ki} + d\xi_{ki}) \right).
\end{aligned}$$

□

With $Q(\boldsymbol{\theta}; \boldsymbol{\theta}_k)$ at hand, we show in the following lemma how $\boldsymbol{\mu}$ and Σ are updated in Step 2.1) of Algorithm 6.1.

Lemma 6.3

Maximizing $Q(\boldsymbol{\theta}; \boldsymbol{\theta}_k)$ with respect to $\boldsymbol{\mu}$ and Σ in Step 2.1) of Algorithm 6.1 gives the next iterates

$$\boldsymbol{\mu}_{k+1} = \frac{\sum_{i=1}^n \delta_{ki} \mathbf{X}_i}{\sum_{i=1}^n \delta_{ki}} \quad \text{and} \quad \Sigma_{k+1} = \frac{1}{n} \sum_{i=1}^n \delta_{ki} (\mathbf{X}_i - \boldsymbol{\mu}_k)(\mathbf{X}_i - \boldsymbol{\mu}_k)^\top. \quad (22)$$

Proof. By Lemma 6.2, $Q(\boldsymbol{\theta}; \boldsymbol{\theta}_k) = Q_{\mathbf{X}|W}(\boldsymbol{\mu}, \Sigma^{-1}; \boldsymbol{\theta}_k) + Q_W(\boldsymbol{\nu}; \boldsymbol{\theta}_k)$ and $\boldsymbol{\mu}$ and Σ do not appear in $Q_W(\boldsymbol{\nu}; \boldsymbol{\theta}_k)$ so that we only need to maximize $Q_{\mathbf{X}|W}(\boldsymbol{\mu}, \Sigma^{-1}; \boldsymbol{\theta}_k)$.

The necessary conditions are $\frac{\partial}{\partial \boldsymbol{\mu}} Q_{\mathbf{X}|W}(\boldsymbol{\mu}, \Sigma^{-1}; \boldsymbol{\theta}_k) = 0$ and $\frac{\partial}{\partial \Sigma^{-1}} Q_{\mathbf{X}|W}(\boldsymbol{\mu}, \Sigma^{-1}; \boldsymbol{\theta}_k) = 0$. Using $\frac{\partial}{\partial \boldsymbol{\mu}} D^2(\mathbf{X}_i; \boldsymbol{\mu}, \Sigma) = -2\Sigma^{-1}(\mathbf{X}_i - \boldsymbol{\mu})$ one obtains that $\frac{\partial}{\partial \boldsymbol{\mu}} Q_{\mathbf{X}|W}(\boldsymbol{\mu}, \Sigma^{-1}; \boldsymbol{\theta}_k) = 0$ if and only if $\sum_{i=1}^n \delta_{ki} \Sigma^{-1}(\mathbf{X}_i - \boldsymbol{\mu}) = 0$. Solving for $\boldsymbol{\mu}$ gives $\boldsymbol{\mu}_{k+1}$ as given in the lemma. For full rank Σ , it holds that $\frac{\partial}{\partial \Sigma^{-1}} \log \det(\Sigma^{-1}) = \Sigma$. Since $\frac{\partial}{\partial \Sigma^{-1}} D^2(\mathbf{X}_i; \boldsymbol{\mu}, \Sigma) = (\mathbf{X}_i - \boldsymbol{\mu})(\mathbf{X}_i - \boldsymbol{\mu})^\top$ one gets $\frac{\partial}{\partial \Sigma^{-1}} Q_{\mathbf{X}|W}(\boldsymbol{\mu}, \Sigma^{-1}; \boldsymbol{\theta}_k) = 0$ if and only if $n\Sigma - \sum_{i=1}^n \delta_{ki} (\mathbf{X}_i - \boldsymbol{\mu})(\mathbf{X}_i - \boldsymbol{\mu})^\top = 0$ which, after solving for Σ , gives the formula for Σ_{k+1} as given in the statement. □

Lemma 6.3 indicates that we need to approximate the weights δ_{ki} , $i = 1, \dots, n$, in Step 2.1) of Algorithm 6.1. Note that

$$dF_{W|\mathbf{X}}(w | \mathbf{x}) = \frac{f_{\mathbf{X}|W}(\mathbf{x} | w) dF_W(w)}{f_{\mathbf{X}}(\mathbf{x})} = \frac{\phi(\mathbf{x}; \boldsymbol{\mu}, w\Sigma)}{f_{\mathbf{X}}(\mathbf{x})} dF_W(w), \quad w > 0,$$

where $\phi(\mathbf{x}; \boldsymbol{\mu}, \Sigma)$ denotes the density of $N_d(\boldsymbol{\mu}, \Sigma)$ so that

$$\begin{aligned}
\delta_{ki} &= \mathbb{E} \left(\frac{1}{W_i} \middle| \mathbf{X}_i; \boldsymbol{\theta}_k \right) = \int_0^\infty \frac{1}{w} dF_{W|\mathbf{X}}(w | \mathbf{X}_i) \\
&= \frac{1}{f_{\mathbf{X}}(\mathbf{X}_i; \boldsymbol{\mu}_k, \Sigma_k, \boldsymbol{\nu}_k)} \int_0^\infty \frac{\phi(\mathbf{X}_i; \boldsymbol{\mu}_k, w\Sigma_k)}{w} dF_W(w; \boldsymbol{\nu}_k).
\end{aligned}$$

This yields

$$\begin{aligned}
 \log(\delta_{ki}) &= \log \left(\int_0^\infty \frac{\phi(\mathbf{X}_i; \boldsymbol{\mu}_k, w \Sigma_k)}{w} dF_W(w; \boldsymbol{\nu}_k) \right) - \log f_{\mathbf{X}}(\mathbf{X}_i; \boldsymbol{\mu}_k, \Sigma_k, \boldsymbol{\nu}_k) \\
 &= \log \left(\int_0^1 \frac{1}{\sqrt{(2\pi)^d F_W^{\leftarrow}(u; \boldsymbol{\nu}_k)^{d+2} |\Sigma_k|}} \exp \left(-\frac{D^2(\mathbf{X}_i; \boldsymbol{\mu}_k, \Sigma_k)}{2F_W^{\leftarrow}(u; \boldsymbol{\nu}_k)} \right) du \right) \\
 &\quad - \log \left(\int_0^1 \frac{1}{\sqrt{(2\pi)^d F_W^{\leftarrow}(u; \boldsymbol{\nu}_k)^d |\Sigma_k|}} \exp \left(-\frac{D^2(\mathbf{X}_i; \boldsymbol{\mu}_k, \Sigma_k)}{2F_W^{\leftarrow}(u; \boldsymbol{\nu}_k)} \right) du \right). \quad (23)
 \end{aligned}$$

Estimation of the latter integral (corresponding to $\log f_{\mathbf{X}}(\mathbf{x})$) was discussed in Algorithm 5.2; the former integral differs from the latter only by a factor of $F_W^{\leftarrow}(u)^{-1}$, and can be estimated similarly; see Remark 5.3 for details.

Summarizing, the k 'th iteration of the algorithm consists of approximating the weights δ_{ki} , $i = 1, \dots, n$ with $\boldsymbol{\nu} = \boldsymbol{\nu}_k$ held fixed (which are then used to update $\boldsymbol{\mu}$ and Σ as in (22)) and then updating $\boldsymbol{\nu}$ by maximizing the original likelihood $\log L^{\text{org}}(\boldsymbol{\theta}; \mathbf{X}_1, \dots, \mathbf{X}_n)$ as a function of $\boldsymbol{\nu}$ with $\boldsymbol{\mu}$ and Σ set to their current estimates, i.e., we set

$$\boldsymbol{\nu}_{k+1} = \underset{\boldsymbol{\nu}}{\operatorname{argmax}} \log L^{\text{org}}(\boldsymbol{\nu}, \boldsymbol{\mu}_{k+1}, \Sigma_{k+1}; \mathbf{X}_1, \dots, \mathbf{X}_n) \quad (24)$$

and solve this $p_{\boldsymbol{\nu}}$ -dimensional optimization problem numerically. This optimization problem is the same optimization problem one would solve if $\boldsymbol{\mu}$ and Σ were known (and given by $\boldsymbol{\mu}_{k+1}$ and Σ_{k+1}) and is a classical ingredient in ECME algorithms; for more details on rates of convergence of the proposed ECME scheme, see Liu and Rubin (1994, Section 4). Note that the dimension $p_{\boldsymbol{\nu}}$ of $\boldsymbol{\nu}$ is typically small so that this optimization problem is also numerically feasible. In our implementation, we use the R optimizer `optim()` which by default only relies on function evaluations and works for non-differentiable functions: Derivative-based methods can, due to small estimation errors in the likelihood function, fail to detect a global optimum.

This step is the most costly one as it involves multiple estimation of the likelihood of the data using Algorithm 5.2: Each call to the likelihood function requires the approximation of n integrals. It turns out that estimating the weights δ_{ki} is faster so that it seems to be fruitful to first update $\boldsymbol{\mu}$ and Σ until convergence (with $\boldsymbol{\nu} = \boldsymbol{\nu}_k$ held fixed) and then update $\boldsymbol{\nu}$. In fact, this can be done efficiently: The weights δ_{ki} depend on \mathbf{X}_i , $\boldsymbol{\mu}_k$ and Σ_k only through the Mahalanobis distances $D^2(\mathbf{X}_i; \boldsymbol{\mu}_k, \Sigma_k)$. Once $\boldsymbol{\mu}_k$ and Σ_k are updated to, say, $\boldsymbol{\mu}'_k$ and Σ'_k , (some of) the new weights δ'_{ki} for the new Mahalanobis distances $D^2(\mathbf{X}_i; \boldsymbol{\mu}'_k, \Sigma'_k)$ can be obtained by interpolating the already calculated weights δ_{ki} corresponding to the (old) Mahalanobis distances $D^2(\mathbf{X}_i; \boldsymbol{\mu}_k, \Sigma_k)$.

It remains to discuss how a starting value $\boldsymbol{\theta}_0$ can be found. We suggest using $\boldsymbol{\mu}_0 = \bar{\mathbf{X}}_n$, the sample mean vector, as an unbiased estimator for $\boldsymbol{\mu}$. Denote by S_n the sample covariance matrix (Wishart matrix) of $\mathbf{X}_1, \dots, \mathbf{X}_n$. Since S_n is unbiased for $\operatorname{cov}(\mathbf{X})$ it follows that $\mathbb{E}(S_n) = \mathbb{E}(W)\Sigma$. The idea is now to maximize the likelihood given $\boldsymbol{\mu} = \boldsymbol{\mu}_0$ and given

6 Fitting multivariate normal variance mixtures

$\Sigma = c \cdot S_n$ with respect to $\boldsymbol{\nu}$ and c (restricted to $c > 0$) which is a $(p_\nu + 1)$ dimensional optimization problem. That is, we find

$$(\boldsymbol{\nu}^*, c^*) = \operatorname{argmax}_{\boldsymbol{\nu}, c > 0} L^{\text{org}}(\boldsymbol{\nu}, \boldsymbol{\mu}_0, cS_n; \mathbf{X}_1, \dots, \mathbf{X}_n) \quad (25)$$

numerically (again via R's `optim()`) and set $\boldsymbol{\nu}_0 = \boldsymbol{\nu}^*$ and $\Sigma_0 = c^* S_n$ which is just a multiple of the Wishart matrix. As this step is merely needed to obtain a starting value for $\boldsymbol{\nu}$ and Σ , this optimization can be done over a subset of the sample $\{\mathbf{X}_1, \dots, \mathbf{X}_n\}$ to save run time.

The complete procedure is summarized in Algorithm 6.4. As convergence criterion we suggest stopping once the maximal relative difference in parameter estimates is smaller than a given threshold. We define the maximal relative difference by

$$d(\boldsymbol{\nu}_k, \boldsymbol{\nu}_{k+1}) = \max_{i=1, \dots, p_\nu} \frac{|\boldsymbol{\nu}_{k,i} - \boldsymbol{\nu}_{k+1,i}|}{|\boldsymbol{\nu}_{k,i}|}, \quad \boldsymbol{\nu}_k = (\boldsymbol{\nu}_{k,1}, \dots, \boldsymbol{\nu}_{k,p_\nu})$$

and similarly for $\boldsymbol{\mu}$ and Σ .

Algorithm 6.4 (ECME algorithm for fitting normal variance mixtures)

Given iid input data $\mathbf{X}_1, \dots, \mathbf{X}_n$ and convergence criteria ε_μ , ε_Σ and ε_ν , estimate $\boldsymbol{\mu}, \Sigma, \boldsymbol{\nu}$ via:

- 1) *Starting value.*
Set $\boldsymbol{\mu}_0 = \bar{\mathbf{X}}_n$ and solve the optimization problem (25) numerically to obtain $\boldsymbol{\nu}^*$ and c^* .
Set $\boldsymbol{\nu}_0 = \boldsymbol{\nu}^*$ and $\Sigma_0 = c^* S_n$.
- 2) *ECME iteration.*
For $k = 0, 1, \dots$, do:
 - 2.1) *Update $\boldsymbol{\mu}$ and Σ .*
Set $\boldsymbol{\mu}_k^{(1)} = \boldsymbol{\mu}_k$ and $\Sigma_k^{(1)} = \Sigma_k$.
For $l = 1, \dots$, do:
 - 2.1.1) Estimate new weights $\delta_{ki}^{(l+1)} = \mathbb{E}(1/W_i | \mathbf{X}_i; \boldsymbol{\mu}_k^{(l)}, \Sigma_k^{(l)}, \boldsymbol{\nu}_k)$, $i = 1, \dots, n$ using (23) and Algorithm 5.2.
 - 2.1.2) Calculate the new iterates $\boldsymbol{\mu}_k^{(l+1)}$ and $\Sigma_k^{(l+1)}$ using (22) with weights $\delta_{ki}^{(l+1)}$, $i = 1, \dots, n$.
 - 2.1.3) If $d(\boldsymbol{\mu}_k^{(l)}, \boldsymbol{\mu}_k^{(l+1)}) < \varepsilon_\mu$ and $d(\Sigma_k^{(l)}, \Sigma_k^{(l+1)}) < \varepsilon_\Sigma$, set $\boldsymbol{\mu}_{k+1} = \boldsymbol{\mu}_k^{(l+1)}$, $\Sigma_{k+1} = \Sigma_k^{(l+1)}$ and go to Step 2.2).
 - 2.2) *Update $\boldsymbol{\nu}$.*
Numerically solve the optimization problem (24) to obtain $\boldsymbol{\nu}_{k+1}$.
 - 2.3) If $d(\boldsymbol{\nu}_k, \boldsymbol{\nu}_{k+1}) < \varepsilon_\nu$, return the MLEs $\boldsymbol{\mu}^* = \boldsymbol{\mu}_{k+1}$, $\Sigma^* = \Sigma_{k+1}$ and $\boldsymbol{\nu}^* = \boldsymbol{\nu}_{k+1}$.

Algorithm 6.4 is implemented in the function `fitnvmix()` of our R package `nvmix`. The mixing variable is specified by providing a function to the argument `qmix`. In the special

7 Numerical Examples

case where W follows an inverse-gamma or Pareto distribution, the density function is known in closed form which is used by `fitnvmix()` when called with argument `qmix = "inverse.gamma"` or `qmix = "pareto"`.

7 Numerical Examples

In this section we provide a careful numerical analysis of all algorithms presented. The first part discusses the type of mixing distributions used; the second, third and fourth part detail numerical examples for estimating the distribution function using Algorithm 4.1 with variable reordering as in Algorithm C.2, estimating the log-density function using Algorithm 5.2, and estimating parameters ν , $\boldsymbol{\mu}$ and Σ given a random sample using Algorithm 6.4, respectively. The last part provides an application of our methods to a multivariate financial data set.

7.1 Test Distributions

For our numerical examples, we consider two distributions for the mixing variable W , an inverse-gamma distribution (so that \mathbf{X} is multivariate t) and a Pareto distribution.

Inverse-gamma mixture Here W follows an inverse-gamma distribution with shape and scale parameter $\nu/2$. The resulting distribution is the multivariate t distribution, $\mathbf{X} \sim \text{MVT}_d(\nu, \boldsymbol{\mu}, \Sigma)$ with positive degrees of freedom ν ; see, for instance, Kotz and Nadarajah (2004, Chapter 1). Note that if $\nu > 1$, $\mathbb{E}(\mathbf{X}) = \boldsymbol{\mu}$ and if $\nu > 2$, $\text{cov}(\mathbf{X}) = \frac{\nu}{\nu-2}\Sigma$. The multivariate t distribution has the density

$$f_{\mathbf{X}}(\mathbf{x}) = \frac{\Gamma((\nu + d)/2)}{\Gamma(\nu/2)\sqrt{(\nu\pi)^d|\Sigma|}} \left(1 + D^2(\mathbf{x}; \boldsymbol{\mu}, \Sigma)/\nu\right)^{-\frac{\nu+d}{2}}, \quad \mathbf{x} \in \mathbb{R}^d. \quad (26)$$

For the ECME procedure it is useful to calculate the weight $\mathbb{E}(1/W \mid \mathbf{X})$. Since

$$f_{W|\mathbf{X}}(w \mid \mathbf{x}) \propto f_{\mathbf{X}|W}(\mathbf{x} \mid w)f_W(w) \propto w^{-\frac{d+\nu}{2}-1} \exp\left(-\frac{(D^2(\mathbf{x}; \boldsymbol{\mu}, \Sigma) + \nu)/2}{w}\right), \quad w > 0,$$

$W \mid \mathbf{X}$ follows an inverse-gamma distribution, i.e., $W \mid \mathbf{X} \sim \text{IG}((d + \nu)/2, (D^2(\mathbf{X}; \boldsymbol{\mu}, \Sigma) + \nu)/2)$. This implies

$$\mathbb{E}(1/W \mid \mathbf{X}) = \frac{\nu + d}{\nu + D^2(\mathbf{X}; \boldsymbol{\mu}, \Sigma)},$$

so that the weights δ_{ki} in Step 2.1.1) of Algorithm 6.4 can be calculated analytically in this case.

7 Numerical Examples

Pareto mixture In order to test our algorithms for a normal variance mixture distribution that has not been studied as extensively as the multivariate t distribution we consider $W \sim \text{Par}(\alpha, x_m)$ with density

$$f_W(w) = \alpha \frac{x_m^\alpha}{w^{\alpha+1}}, \quad w \geq x_m.$$

One can calculate that $\mathbb{E}(W^k)$ exists with $\mathbb{E}(W^k) = \alpha/(\alpha - k)$ if $k < \alpha$. This implies for the resulting normal variance mixture $\mathbf{X} = \boldsymbol{\mu} + \sqrt{W}\mathbf{A}\mathbf{Z}$ that $\mathbb{E}(\mathbf{X}) = \boldsymbol{\mu}$ for $\alpha > 1/2$ and $\text{cov}(\mathbf{X}) = \frac{\alpha}{\alpha-1}\Sigma$ for $\alpha > 1$. The density $f_{\mathbf{X}}(\mathbf{x}) = f_{\mathbf{X}}(\mathbf{x}; \boldsymbol{\mu}, \Sigma, \alpha, x_m)$ can be determined using (4):

$$\begin{aligned} f_{\mathbf{X}}(\mathbf{x}) &= \frac{\alpha x_m^\alpha}{\sqrt{(2\pi)^d |\Sigma|}} \int_{x_m}^{\infty} w^{-d/2-\alpha-1} \exp\left(-\frac{D^2(\mathbf{x}; \boldsymbol{\mu}, \Sigma)}{2w}\right) dw \\ &= \frac{\alpha x_m^\alpha}{\sqrt{(2\pi)^d |\Sigma|}} \left(\frac{D^2(\mathbf{x}; \boldsymbol{\mu}, \Sigma)}{2}\right)^{-d/2-\alpha} \int_0^{\frac{D^2(\mathbf{x}; \boldsymbol{\mu}, \Sigma)}{2x_m}} u^{d/2+\alpha-1} \exp(-u) du \\ &= \frac{\alpha x_m^\alpha}{\sqrt{(2\pi)^d |\Sigma|}} \left(\frac{D^2(\mathbf{x}; \boldsymbol{\mu}, \Sigma)}{2}\right)^{-d/2-\alpha} \gamma\left(\alpha + \frac{d}{2}; \frac{D^2(\mathbf{x}; \boldsymbol{\mu}, \Sigma)}{2x_m}\right), \quad \mathbf{x} \in \mathbb{R}^d, \end{aligned}$$

where $\gamma(z; x) = \int_0^x t^{z-1} e^{-t} dt$ for $z, x > 0$ denotes the (lower) incomplete gamma function. Note that $f_{\mathbf{X}}(\mathbf{x}; \boldsymbol{\mu}, \Sigma, \alpha, x_m) = f_{\mathbf{X}}(\mathbf{x}; \boldsymbol{\mu}, x_m \Sigma, \alpha, 1)$ so that the scale parameter x_m is redundant as the scaling can be achieved via scaling Σ . We can thus set $x_m = 1$ and obtain

$$f_{\mathbf{X}}(\mathbf{x}; \boldsymbol{\mu}, \Sigma, \alpha) = \frac{\alpha}{\sqrt{(2\pi)^d |\Sigma|}} \left(\frac{D^2(\mathbf{x}; \boldsymbol{\mu}, \Sigma)}{2}\right)^{-d/2-\alpha} \gamma\left(\alpha + \frac{d}{2}; \frac{D^2(\mathbf{x}; \boldsymbol{\mu}, \Sigma)}{2}\right), \quad \mathbf{x} \in \mathbb{R}^d. \quad (27)$$

We use the notation $\mathbf{X} \sim \text{PNVM}(\alpha, \boldsymbol{\mu}, \Sigma)$ (“Pareto normal variance mixture”) for a random vector \mathbf{X} with density (27).

As in the case of an inverse-gamma mixture, it is possible to derive an expression for $\mathbb{E}(1/W \mid \mathbf{X})$ in the Pareto setting. Note that

$$f_{W|\mathbf{X}}(w \mid \mathbf{x}) \propto f_{\mathbf{X}|W}(\mathbf{x} \mid w) f_W(w) \propto w^{-(\alpha+d/2+1)} \exp\left(-D^2(\mathbf{x}; \boldsymbol{\mu}, \Sigma)/(2w)\right), \quad w > 1,$$

so that using the density transformation formula we obtain for $\tilde{W} = 1/W$ that

$$f_{\tilde{W}|\mathbf{X}}(\tilde{w} \mid \mathbf{x}) \propto \tilde{w}^{\alpha+d/2-1} \exp(-\tilde{w} D^2(\mathbf{x}; \boldsymbol{\mu}, \Sigma)/2), \quad \tilde{w} \in (0, 1).$$

Therefore, $W^{-1} \mid \mathbf{X}$ follows a $(0, 1)$ truncated gamma distribution with shape $\alpha + d/2$ and scale $2/D^2(\mathbf{X}; \boldsymbol{\mu}, \Sigma)$. For more details on truncated gamma distributions, see Coffey and Muller (2000); Equation (2.12) therein implies that

$$\mathbb{E}(1/W \mid \mathbf{X}) = \frac{F_{\Gamma}(1; \alpha + d/2 + 1, 2/D^2(\mathbf{X}; \boldsymbol{\mu}, \Sigma))}{F_{\Gamma}(1; \alpha + d/2, 2/D^2(\mathbf{X}; \boldsymbol{\mu}, \Sigma))} \frac{2\alpha + d}{D^2(\mathbf{X}; \boldsymbol{\mu}, \Sigma)}.$$

7 Numerical Examples

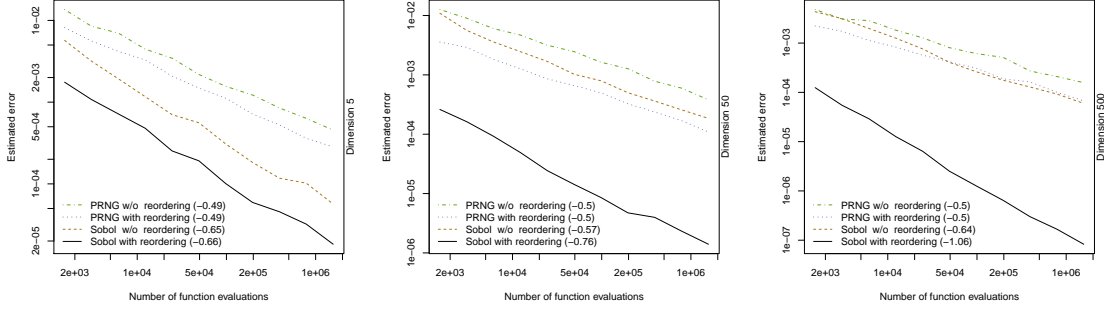


Figure 2 Average absolute errors of different estimators for $F_{\mathbf{X}}(\mathbf{x})$ as a function of n for $\mathbf{X} \sim \text{MVT}_d(2, \mathbf{0}, \Sigma)$, where for each n , 15 different settings for Σ and \mathbf{x} are randomly chosen. Regression coefficients are in parentheses in the legends.

7.2 Estimating the distribution function

In the case where $\mathbf{X} \sim \text{MVT}_d(\nu, \boldsymbol{\mu}, \Sigma)$, Algorithm 4.1 combined with the variable reordering Algorithm C.2 can be used to estimate $F(\mathbf{a}, \mathbf{b})$, and is implemented in the function `pStudent()` in the R package `nvmmix`. In this case, one can also use the QRSVN algorithm from Genz and Bretz (2002), which is implemented in the function `pmvt()` of the R package `mvtnorm` (Genz, Bretz, et al. (2019)). The differences between these two algorithms was explained in Section 3. Furthermore, our implementation relies on C code, whereas `pmvt()` internally calls Fortran code.

7.2.1 Error behaviour as a function of the sample size

In order to assess the performance of our algorithm let us first consider estimated absolute errors as a function of the number of function evaluations. Four settings are considered: (pure) MC with and without reordering and RQMC (using a randomized Sobol' sequence) with and without reordering. In Figures 2 and 3, estimated absolute errors (estimated as in Algorithm 4.1 via $\hat{\varepsilon}$ in Step 4.3)) are reported for different sample sizes n (which refer to the total number of function evaluations) in different dimensions using the four aforementioned methods for the multivariate t case and the Pareto mixture. For each dimension and for each n we report the average estimated absolute error for 15 different parameter settings. In each parameter setting, an upper limit is randomly chosen via $\mathbf{b} \sim \text{U}(0, 3\sqrt{d})^d$ and a correlation matrix R is sampled as a standardized Wishart matrix via the function `rWishart()` in R. The lower limit is set to $\mathbf{a} = (-\infty, \dots, -\infty)$. The degrees of freedom ν in the MVT setting and the shape parameter α in the PNVM setting are set to 2.

It is evident that RQMC methods yield lower errors than their MC counterparts. We also report the convergence speed (as measured by the regression coefficient α of $\log \hat{\varepsilon} = \alpha \log n + c$ displayed in the legend): Variable reordering does not have an influence on the convergence

7 Numerical Examples

speed $1/\sqrt{n}$ of MC methods; however, it does speed up the RQMC methods. A possible explanation is that variable reordering can reduce the effective dimension. This is discussed below in more detail.

7.2.2 The effect of variable reordering

Investigating the variance of the integrand It is interesting to further investigate the effect of variable reordering as detailed in Section 4.2. To this end, the variance of the integrand g from (15) given by

$$\text{var}(g(\mathbf{U})) = \int_{[0,1]^d} g^2(\mathbf{u}) d\mathbf{u} - \left(\int_{[0,1]^d} g(\mathbf{u}) d\mathbf{u} \right)^2$$

is estimated, once with the original g without reordering, and once with \tilde{g} which is the integrand g after applying Algorithm C.2 to the inputs $\mathbf{a}, \mathbf{b}, \Sigma$. We use a randomized experiment and do the following 50 000 times for an inverse-gamma mixture: Sample $d \sim U(\{5, \dots, 500\})$, $\nu \sim U(0.1, 5)$ and $\mathbf{a}, \mathbf{b}, \Sigma$ are randomly chosen as in the previous section. The variance of the integrand is then estimated via the sample variance of $g(\mathbf{U}_1), \dots, g(\mathbf{U}_N)$ for $N = 10\,000$. Results can be found in Figure 4: On the left, variances have been ordered according to the ordering of the variances when variable reordering is employed (for better visibility of the reordering effect). On the right, a density plot of the ratios $\text{var}(\tilde{g}(\mathbf{U}))/\text{var}(g(\mathbf{U}))$ is shown. It can be confirmed that in the vast majority of cases, variable reordering substantially decreases the variance of the integrand. In only 12 of the 50 000 runs did the estimated variance after reordering exceed the variance without reordering.

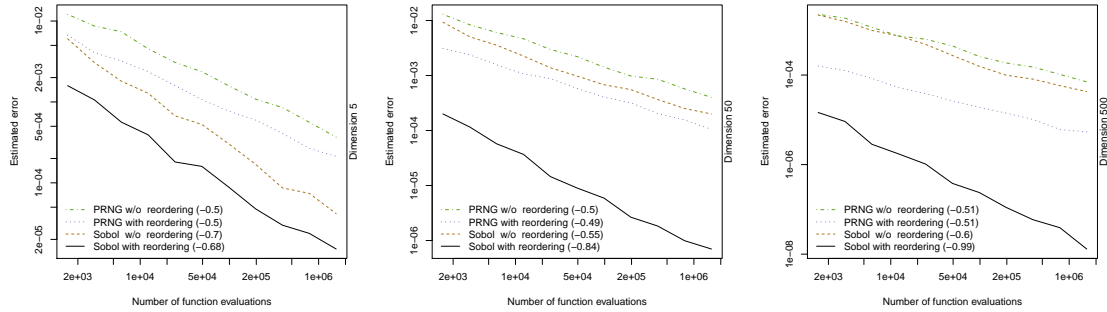


Figure 3 Average absolute errors of different estimators for $F_{\mathbf{X}}(\mathbf{x})$ as a function of n for $\mathbf{X} \sim \text{PNVM}_d(2, \mathbf{0}, \Sigma)$, where for each n , 15 different settings for Σ and \mathbf{x} are randomly chosen. Regression coefficients are in parentheses in the legends.

7 Numerical Examples

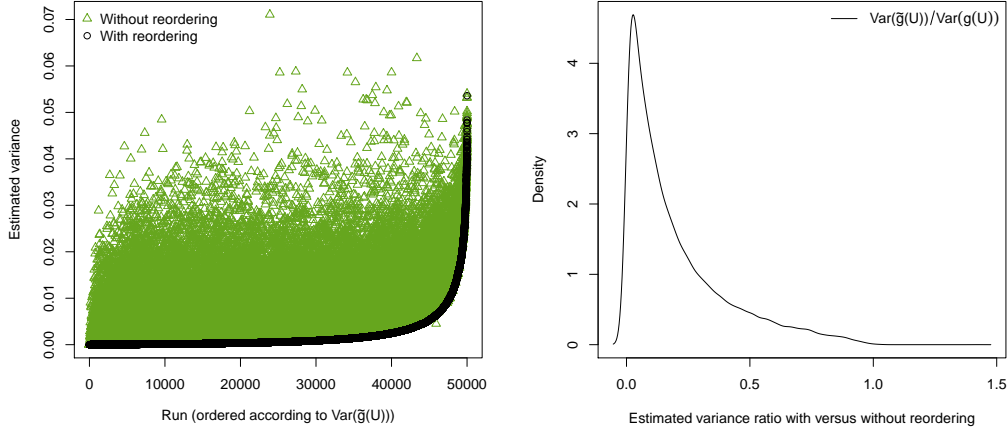


Figure 4 Left: Variance of the integrand $\text{var}(g(\mathbf{U}))$ with and without variable reordering. Right: Density plot of estimated variance ratios.

Effective dimension of the integrand As was seen in Figures 2 and 3, reordering improves both MC and RQMC methods; the effect is however stronger for RQMC methods. A possible explanation for this is that the variable reordering not only reduces the overall variance of the integrand, $\sigma^2 = \text{var}(g(\mathbf{U}))$, as seen in the previous part, but also the *effective dimension* of the integrand, to be defined later. (R)QMC methods often work better if only a small number of variables are important, see Wang and Fang (2003) and references therein for a discussion and examples. Variable reordering, as explained in Section 4.2, was derived in a way such that the first components are the most important ones.

Sensitivity indices, such as Sobol' indices, can help understand the importance of different variables of an integrand. Following Lemieux (2009, Ch. 6.3) and Sobol' (2001), we consider the ANOVA decomposition of a (square integrable) function $g : (0, 1)^d \rightarrow \mathbb{R}$ given by

$$g(\mathbf{u}) = \sum_{I \subseteq \{1, \dots, d\}} g_I(\mathbf{u})$$

where

$$g_I(\mathbf{u}) = \int_{[0,1]^{d-k}} g(\mathbf{u}) d\mathbf{u}_{-I} - \sum_{J \subset I} g_J(\mathbf{u}), \quad g_\emptyset(\mathbf{u}) = \int_{[0,1]^d} g(\mathbf{u}) d\mathbf{u};$$

here, $k = |I|$ and \mathbf{u}_{-I} is the vector \mathbf{u} without components $k \in I$. The g_I 's only depend on variables $i \in I$ and are orthogonal; if $I \neq \emptyset$, g_I has mean zero. The overall variance of the integrand can then be decomposed as $\sigma^2 = \text{var}(g(\mathbf{U})) = \sum_{I \subseteq \{1, \dots, d\}} \sigma_I^2$ where $\sigma_I^2 = \text{var}(g_I(\mathbf{U})) = \int_{[0,1]^d} g_I(\mathbf{u})^2 d\mathbf{u}$. The number

$$S_I = \frac{\sigma_I^2}{\sigma^2} \in [0, 1]$$

7 Numerical Examples

is called *Sobol' index* of I . It explains the fraction of the overall variance of the integrand explained by the variables in I ; if this number is close to 1, it means that most of the variance is explained by g_I and therefore by the variables in I . If $I = \{l\}$ is a singleton, $S_I = S_l$ is called a *first order index*.

Another useful sensitivity index is the *total effect index* of variable $l \in \{1, \dots, d\}$ given by

$$S_{T_l} = \frac{1}{\sigma^2} \sum_{I \subseteq \{1, \dots, d\}: l \in I} \sigma_I^2$$

which measures the relative impact of component l and all its interactions. Care must be taken when interpreting this value as $\sum_{i=1}^d S_{T_i} \geq 1$ in general since interactions are counted several times. For instance, $\sigma_{\{1,2\}}^2$ is contained in S_{T_1} as well as in S_{T_2} .

Finally, the *effective dimension in the superposition sense* in proportion $p \in (0, 1]$ is the smallest integer d_S so that

$$\frac{1}{\sigma^2} \sum_{I: |I| \leq d_S} \sigma_I^2 \geq p.$$

If the effective dimension is d_S , the integrand can be well approximated by functions of at most d_S variables; see Lemieux (2009, Sec. 3.6.1).

The indices $S_{\{l\}}$ and S_{T_l} for $l \in \{1, \dots, d\}$ can be estimated using Owen (2013)'s method which is implemented in the function `sobolowen()` in the R package `sensitivity`; see Pujol et al. (2017). Figure 5 shows estimated Sobol' indices in two settings: In each setting, $W \sim \text{IG}(1/2, 1/2)$ (so that \mathbf{X} follows a multivariate t distribution with 1 degrees of freedom) and $d = 10$. The upper limit \mathbf{b} and the scale matrix Σ were found by trial & error so that there is either a substantial variance reduction (top figure) achieved by reordering or an increase in variance (bottom figure). In order to be consistent with the definition of the integrand g in (15), variables are called $0, \dots, d-1$ so that they correspond to u_0, \dots, u_{d-1} . For instance, in the top figure, one can read that $S_{\{0\}} \approx 0.52$ after reordering so that 52% of the variance of g can be explained by a function $g_{\{0\}}(u_0)$.

Inspecting the top figures where variable reordering led to a decrease in variance of approximately 99% reveals that both first order and total effect indices are decreasing in the dimension after variable reordering was performed. Also, the figure label includes the sum of the first order indices. After reordering, 65% (as opposed to 15%) of the overall variance of the integrand is explained by components g_I of g of exactly one variable, hinting at the fact that the effective dimension decreased: The effective dimension in the superposition sense in proportion 65% decreased to 1 after reordering.

There are rare cases when variable reordering leads to an increase in variance: In the bottom figures, the relative increase is about 31%. Here, the new ordering is clearly not optimal and indices are not decreasing with the dimension. Given the nature of the greedy procedure it is expected that in some cases, no improvement is achieved.

7 Numerical Examples

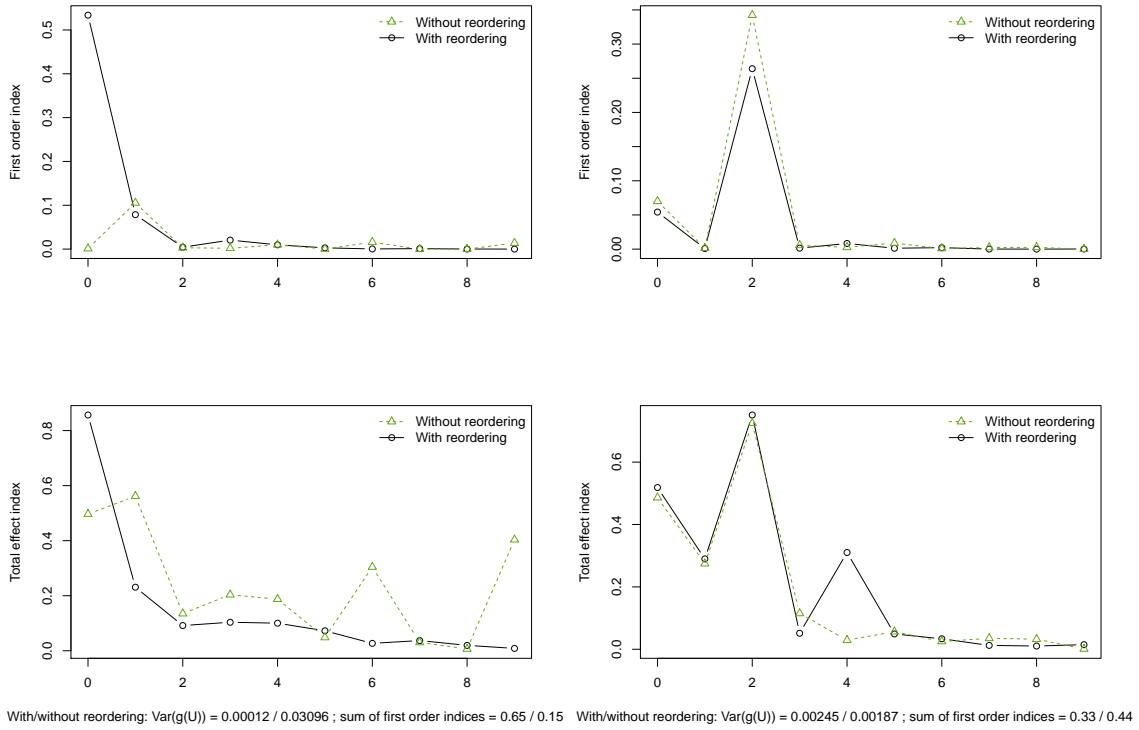


Figure 5 Estimated first order and total effect indices with and without reordering for an inverse-gamma mixture in a setting with high variance reduction (top) and increase in variance (bottom).

7.2.3 Run times

In this part we take a brief look at the run-times of Algorithm 4.1 combined with the variable reordering Algorithm C.2. We restrict our attention to the important multivariate t case and compare run times of our implementation in `pStudent()` with the run times of the above mentioned QRSVN algorithm described in Genz and Bretz (2002) and provided by the function `pmvt()` in the R package `mvtnorm`.

In order to get meaningful estimates of the CPU time, for each dimension d , the following is done 15 times: Sample \mathbf{b} and Σ as before when estimating $\text{var}(g(\mathbf{U}))$, set $\mathbf{a} = (-\infty, \dots, -\infty)$ and $\nu = 2$. Then call `pmvt()` and `pStudent()` three times each and average their CPU times obtained using the package `microbenchmark` of Mersmann (2015). The above procedure is done for an absolute error tolerance $\varepsilon = 0.001$ and the maximum number of function evaluations is chosen such that both algorithms always terminate with the correct precision.

Figure 6 shows the run times obtained. The symbols represent the corresponding means whereas the lines show the largest/smallest CPU time measured for that dimension. Note

7 Numerical Examples

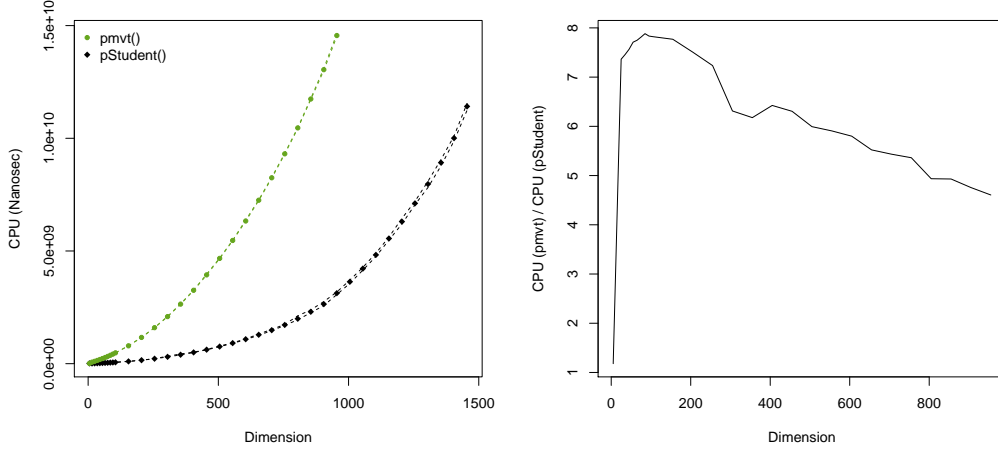


Figure 6 Run times based on three replications of 15 randomly chosen inputs \mathbf{b} and Σ in each dimension (left); run-time ratios relative to `pStudent()` (right).

that `pmvt()` only works for dimensions up to 1000. Figure 6 shows that our implementation significantly outperforms the existing standard which takes up to 8 times more run time.

7.3 Estimating the density function

In this section we test the performance of Algorithm 5.2 to estimate the log-density of $\mathbf{X} \sim \text{MVT}_d(\nu, \boldsymbol{\mu}, \Sigma)$ and $\mathbf{X} \sim \text{PNVM}_d(\alpha, \boldsymbol{\mu}, \Sigma)$. Note that the density is known in either case and given in (26) and (27) so that estimated and true log-density values can be compared.

We sample $n = 1000$ points from $\mathbf{X} \sim \text{MVT}_d(\nu = 1, \mathbf{0}, I_d)$ in dimension $d = 10$ and evaluate the density of $\text{MVT}_d(\nu = 4, \mathbf{0}, I_d)$ at the sampled points. The Pareto case is done similarly. Figure 7 displays results obtained by the adaptive algorithm (Algorithm 5.2) and by the crude (non-adaptive) Algorithm C.1; the true log-density and the probability $\mathbb{P}(D^2(\mathbf{X}, \mathbf{0}, I_d) > m^2)$ are also plotted. The latter probability gives an idea of how likely it is to see a sample point \mathbf{x} with Mahalanobis distance greater than m . For small Mahalanobis distances, both algorithms perform well. For larger ones the problem becomes harder as the underlying integrand becomes more difficult to integrate (recall Figure 1 and the discussion thereafter) and the crude, non-adaptive version gives highly biased results. The adaptive version, however, is able to accurately estimate the log-density for any Mahalanobis distance and is furthermore much faster (it takes only approximately 1 second for a total of $n = 1000$ log-density estimations).

By inspecting the axes in Figure 7, one can see that our procedure performs well even for very large Mahalanobis distances that would rarely be observed. For likelihood-based

7 Numerical Examples

methods, such as Algorithm 6.4, it is, however, crucial to be able to evaluate the density function for a wide range of inputs. For instance, consider the problem where a sample $\mathbf{X}_1, \dots, \mathbf{X}_n \stackrel{\text{ind.}}{\sim} \text{MVT}_d(\nu, \mathbf{0}, I_d)$ for unknown ν is given. It is then necessary to evaluate the log-density of $\mathbf{X}_1, \dots, \mathbf{X}_n$ at a range of values of ν in order to find the maximum likelihood estimator. In fact, this was the motivation for performing the experiments undertaken to produce Figure 7: The sample is coming from a heavy-tailed multivariate t distribution and the log-density function of a less heavy tailed multivariate t distribution is evaluated at that sample. The same intuition lies behind the experiment to produce the plot on the right of Figure 7.

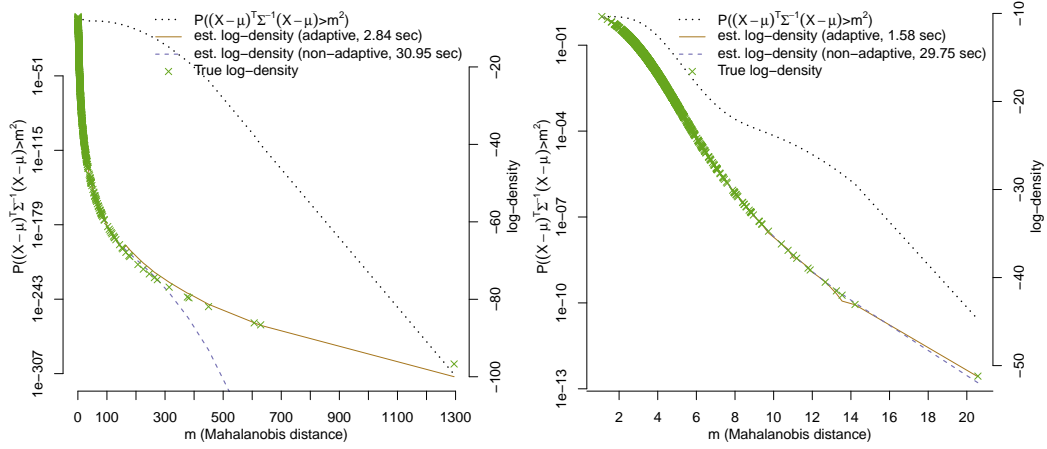


Figure 7 Estimated log-density of $\text{MVT}_d(\nu = 4, \mathbf{0}, I_d)$ (left) and $\text{PNVM}_d(\alpha = 6, \mathbf{0}, I_d)$ (right) in $d = 10$ evaluated at $n = 1000$ points sampled from $\text{MVT}_d(\nu = 1, \mathbf{0}, I_d)$ (left) and $\text{PNVM}(\alpha = 2, \mathbf{0}, I_d)$ (right).

7.4 Fitting normal variance mixture distributions

In this section we provide examples for our fitting procedure Algorithm 6.4. While in the special case where W follows an inverse-gamma distribution (i.e., $\mathbf{X} \sim \text{MVT}_d(\nu, \boldsymbol{\mu}, \Sigma)$ for which the joint density function is available in closed form), ECME methods described in Liu and Rubin (1995) and Nadarajah and Kotz (2008) can be applied directly (implemented, for instance, in the function `fit.mst()` in the R package `QRM`; see Pfaff and McNeil (2016)), this is not the case for a general normal variance mixture distribution where the density function may not be available in closed form. In the latter case, we do rely on Algorithm 6.4 in combination with our adaptive procedure described in Algorithm 5.2 to estimate the log-density function. This is all done automatically in the function `fitnvmix()` which merely needs a specification of the mixing distribution in the form of its quantile function.

7 Numerical Examples

As in the previous section, we consider an inverse-gamma and a Pareto mixture as test cases. We chose these two distributions where the density function is known in closed form so that we are able to investigate if optimizing the log-likelihood estimated via Algorithm 5.2 (as opposed to using a closed formula for the log-likelihood) has a significant effect on parameter estimates. In a practical setting where the density function is not known in closed form (as is the case for the inverse-Burr mixture considered in the data analysis) such comparison is not possible.

Our algorithm is tested in dimensions $d \in \{10, 50\}$ for sample sizes n between 250 and 5 000. In each setting, n random vectors $\mathbf{X}_1, \dots, \mathbf{X}_n \stackrel{\text{ind.}}{\sim} \text{MVT}_d(\nu = 2.5, \mathbf{0}, \Sigma)$ are sampled and then Algorithm 6.4 is used to estimate the parameters. We randomly choose Σ as DRD where R is a random Wishart matrix and D is diagonal with entries $D_{ii} \stackrel{\text{ind.}}{\sim} \text{U}(2, 5)$ for $i = 1, \dots, d$. Results are displayed in Figure 8 where the estimate $\hat{\nu}$ of ν is plotted as a function of the number of ECME iterations (see Step 2) of Algorithm 6.4). The optimizations in Steps 1) and 2.2) of Algorithm 6.4 are based on the estimated log-likelihood function via Algorithm 5.2.

As mentioned earlier, an ECME procedure for estimating parameters of a multivariate t distribution is available in the function `fit.mst()`. The symbols at the end of the curves in Figure 8 denote estimates obtained from this function. It can be confirmed that not only does our procedure converge to the correct maximum likelihood estimate in the given examples, but also that run times are reasonably small for this challenging problem. Note that only few iterations are needed until convergence is detected.

A similar experiment is performed for the Pareto-mixture case, see Figure 9. Here, the symbols at the end of each line display results obtained from Algorithm 6.4 using analytical weights and densities, obtained by calling our function `fitnvmix()` with `qmix = "pareto"`.

The run times displayed in Figures 8 and 9 may seem counter-intuitive; however, several factors influence run time: The larger the sample size n , the more integrals need to be approximated and the higher the probability of observing extreme Mahalanobis distances. Furthermore, the problem of estimating the log-density and the weights becomes harder the larger the Mahalanobis distance of the input. However, larger sample sizes can also lead to a quicker convergence of the weights in Step 2.1) of Algorithm 6.4 and also to faster convergence of the estimates of the mixing variable in Step 2.2) of Algorithm 6.4. Overall, as there are numerical approximations involved at many levels, it will depend on the sample at hand how long the algorithm takes. This explains why run times are not monotone in the sample size n .

7.5 Example application

This section demonstrates an application of all our methods presented to a real financial data set. We consider daily return data of 5 constituents of the SP500 index between 2007-01-03 and 2009-12-31 ($n = 755$ data points in $d = 5$). The dataset `SP500` is obtained from the R package `qrmdata`, see Hofert and Hornik (2016), and the stocks considered are AAPL (Apple), ADBE (Adobe), INTC (Intel), ORCL (Oracle) and GOOGL (Google). We first fit

7 Numerical Examples

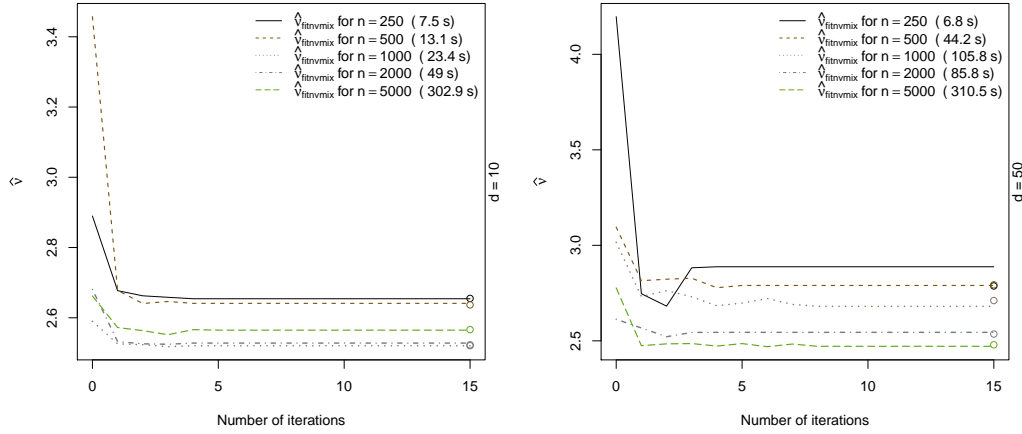


Figure 8 Estimates $\hat{\nu}$ computed by Algorithm 6.4 as a function of the number of ECME iterations for multivariate t distributions of different sample sizes and dimensions. The symbols at the end of each curve denote the maximum likelihood estimator of ν as found by the ECME algorithm with analytical weights and densities.

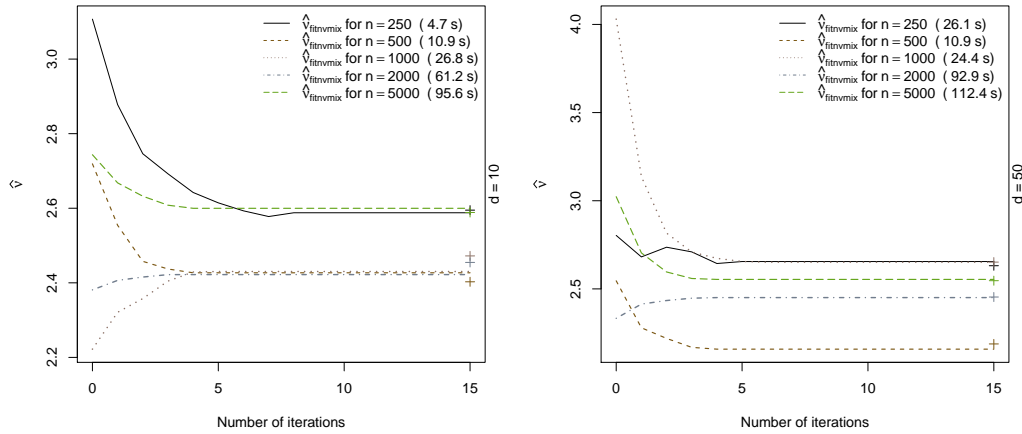


Figure 9 Estimates $\hat{\nu}$ computed by Algorithm 6.4 as a function of the number of ECME iterations for Pareto mixture distributions of different sample sizes and dimensions. The symbols at the end of each curve denote the maximum likelihood estimator of ν as found by the ECME algorithm with analytical weights and densities.

marginal ARMA(1, 1) – GARCH(1, 1) models and then fit normal variance mixture models to the standardized residuals (“innovations”).

7 Numerical Examples

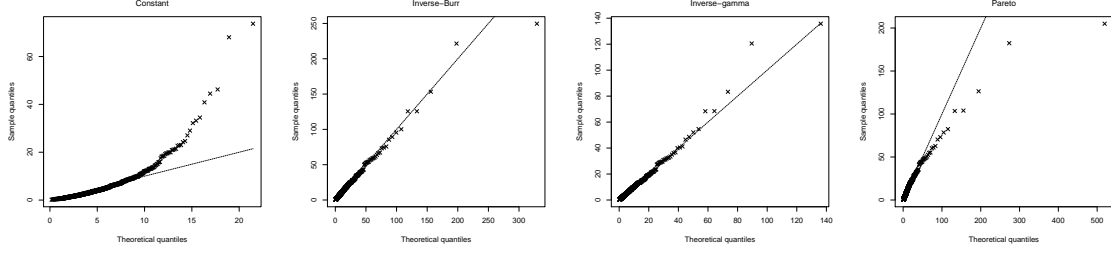


Figure 10 Q-Q Plots of the empirical quantiles of the Mahalanobis distances $D^2(\mathbf{x}_i, \hat{\boldsymbol{\mu}}, \hat{\boldsymbol{\Sigma}})$, $i = 1, \dots, n$, versus their theoretical quantiles for different models using a 5 stock portfolio with data from the SP500 data set.

Four normal variance mixture models are considered: The multivariate t (an inverse-gamma mixture), a Pareto-mixture, an inverse-Burr mixture and the multivariate normal, where \mathbf{X} follows an inverse-Burr mixture if $F_W^{\leftarrow}(u, \boldsymbol{\nu}) = (u^{-1/\nu_2} - 1)^{-1/\nu_1}$ (which is the quantile function of $1/\tilde{W}$ where $\tilde{W} \sim \text{Burr}(\nu_1, \nu_2)$ has distribution function $F_{\tilde{W}}(\tilde{w}) = 1 - (1 + \tilde{w}^{\nu_1})^{-\nu_2}$ for $\tilde{w} > 0$ and $\nu_1, \nu_2 > 0$). We highlight that in the inverse-Burr mixture case, neither the density of the resulting mixture nor weights for our estimation procedure are available in closed form, so that in this case, we indeed rely on our adaptive estimation procedure Algorithm 5.2 to estimate the log-density function. As such, we supply aforementioned quantile function as a “black box” to our fitting procedure via `fitnvmix(, qmix = function(u, nu) (u^(-1/nu[2]) - 1)^(-1/nu[1]))`. We remark that the multivariate normal case is trivial from an estimation point of view, as the maximum likelihood estimators for $\boldsymbol{\mu}$ and $\boldsymbol{\Sigma}$ are merely the sample mean and the sample variance, respectively; this case is included for the sake of comparison.

We fit the aforementioned distributions to the stock data using Algorithm 6.4. For the inverse-gamma and Pareto-mixtures we find $\hat{\nu} = 5.65$ and $\hat{\nu} = 1.64$, respectively, when using the closed form densities and weights; if weights and densities are estimated, we found $\hat{\nu} = 5.62$ (20 sec) and $\hat{\nu} = 1.61$ (13 sec), respectively. Overall it is reassuring that the estimates obtained from analytical and estimated weights and densities only differ slightly; given the difficulty of the problem the run times also seem reasonable. For the inverse-Burr mixture, we found $\hat{\boldsymbol{\nu}} = (2.15, 3.61)$ after 30 seconds run-time.

Figure 10 displays Q-Q Plots of $D^2(\mathbf{x}_i, \hat{\boldsymbol{\mu}}, \hat{\boldsymbol{\Sigma}})$, $i = 1, \dots, n$ as a graphical goodness-of-fit test. Theoretical quantiles are estimated using the methods described in Section B. Clearly, the multivariate normal distribution (corresponding to constant W) provides a poor fit to the data as the tail is heavily underestimated. Both the inverse-gamma mixture and the inverse-Burr mixture provide an excellent fit to the data; the Pareto-mixture however shows too heavy tails. These plots confirm our main motivation outlined in the introduction: The multivariate normal is poorly suited for heavy-tailed return-data; normal variance mixtures, however, are more flexible in that they allow for heavier joint tails, often giving a better fit.

8 Conclusion

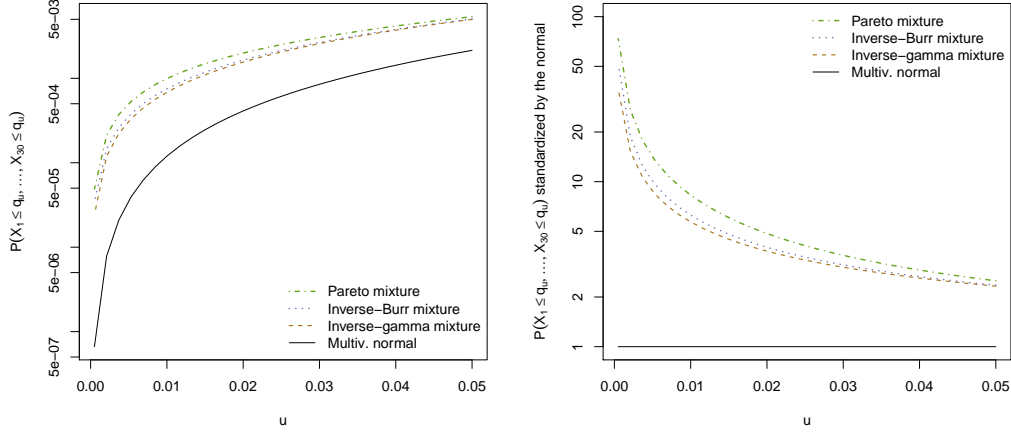


Figure 11 Estimated shortfall probabilities for different models for a 5 stock portfolio with data from the SP500 data set (left); same probabilities standardized by the normal case (right).

Finally, we use Algorithm 4.1 to estimate the joint quantile shortfall probability

$$Q(u) := \mathbb{P}(X_1 \leq F_{X_1}^{\leftarrow}(u), \dots, X_d \leq F_{X_d}^{\leftarrow}(u))$$

for $u \in (0, 1)$. In our context this is the probability that each of the 5 stocks yields a return smaller than its respective u quantile; for small u , $Q(u)$ is the probability of a joint large loss and a rare event. This quantity is often considered in risk management to quantify the risk associated with joint extreme events. Since the margins are continuous, $Q(u)$ is the underlying copula evaluated at (u, \dots, u) . In Figure 11 we plot the estimated quantile shortfall probability $Q(u)$ for a range of values of u for each fitted model separately. The figure on the right-hand-side shows the same probabilities $Q(u)$ standardized by the corresponding normal probability. The plots show again that the Pareto-mixture is significantly more heavy tailed than the multivariate t distribution: It yields significantly higher shortfall probabilities. Furthermore these plots exemplify that our Algorithm 4.1 is also capable of estimating small probabilities despite the increasing numerical difficulty when moving outwards in the joint tail.

8 Conclusion

We introduced efficient algorithms to perform the four main tasks for multivariate normal variance mixtures: Estimating the distribution function, the log-density function, sampling and estimating parameters for a given data set when only the quantile function of the mixing variable W is available. Due to the importance of multivariate normal variance

8 Conclusion

mixtures for disciplines such as actuarial science or quantitative risk management, these algorithms are also widely applicable in practice.

We saw that the distribution function and the log-density function of normal variance mixtures can be accurately and quickly estimated even in high dimensions using RQMC algorithms. The algorithm for the distribution function relies on a generalization of methods that were used for estimating multivariate normal and t probabilities in the past, including an efficient variable reordering algorithm. The algorithm for the log-density is based on an adaptive RQMC procedure that samples only in important regions. We also saw that it is possible to fit multivariate normal variance mixtures using an ECME algorithm in such generality where all involved quantities such as log-densities and weights need to be estimated via RQMC methods. Numerical results validate our methods. An implementation of all methods is provided in the R package `nvmmix`.

We remark that our work also exemplifies the superiority of RQMC methods even in very high dimensions over MC methods for this class of problems.

Another application of our methods is related to normal variance mixture copulas, the implicit copulas derived from normal variance mixture distributions. These copulas can be used to build flexible models with different joint and marginal behaviours. The methods presented here can be used directly to evaluate the distribution and log-density function and for sampling; corresponding methods are implemented in the R package `nvmmix`, too.

A possible limitation of our methods is the assumption of a computationally tractable quantile function of the mixing variable W . For more complicated distributions such quantile function may not be available so that an avenue for future research could be to modify our methods so that they work with a random number generator (RNG) for W (for instance, based on acceptance-rejection algorithms). While sampling and estimating the distribution function is possible when instead of the quantile function of W a RNG for W is provided, this is not the case for estimating the log-density (and thus for the fitting procedure) as our methods are adaptive and thus require sampling in certain low-probability subregions of the support of W .

We also demonstrated via a few examples how variable reordering affects Sobol' indices of the integrand and therefore the effective dimension; given by how much the reordering improves the performance of our RQMC estimator for the distribution function, we believe it would be interesting to explore if this idea can be exploited in other problems as well.

A Evaluation of singular normal variance mixtures

If $\Sigma \in \mathbb{R}^{d \times d}$ is positive semidefinite with rank $1 \leq r < d$, the resulting singular normal variance mixture can be estimated by applying results described in Genz and Kwong (2000), who developed an accurate method to evaluate the distribution function of a multivariate normal distribution with singular correlation matrix Σ , see also Genz and Bretz (2009, Section 5.2) for more details.

Let $\Sigma = CC^\top$ with $C_{ij} = 0$ for $j > r$, $i = 1, \dots, d$, that is, C is lower triangular with some diagonal elements being zero; see Healy (1968) for an algorithm to compute such C which uses a numerical tolerance to determine zero-entries. After permutations and scalings (that must also be applied to \mathbf{a} and \mathbf{b}), C shall have the following form where “*” denotes an entry that can be zero or non-zero:

$$C = \begin{pmatrix} 1 & 0 & 0 & \dots & \dots & \dots & \dots & 0 \\ \vdots & \vdots & \vdots & \vdots & \vdots & \vdots & \vdots & \vdots \\ 1 & 0 & \dots & \dots & \dots & \dots & \dots & 0 \\ * & 1 & 0 & \dots & \dots & \dots & \dots & 0 \\ \vdots & \vdots & \vdots & \vdots & \vdots & \vdots & \vdots & \vdots \\ * & 1 & 0 & \dots & \dots & \dots & \dots & 0 \\ \vdots & \vdots & \vdots & \vdots & \vdots & \vdots & \vdots & \vdots \\ * & * & \dots & * & 1 & 0 & \dots & 0 \\ \vdots & \vdots & \vdots & \vdots & \vdots & \vdots & \vdots & \vdots \\ * & * & \dots & * & 1 & 0 & \dots & 0 \end{pmatrix} \begin{matrix} 1 \\ \vdots \\ k_1 \\ 1 \\ \vdots \\ k_2 \\ \vdots \\ 1 \\ \vdots \\ k_r \end{matrix}$$

Note that $\sum_{j=1}^r k_j = d$. Define $m_i = \sum_{j=1}^{i-1} k_j$ with $m_1 = 0$. As demonstrated in Genz and Kwong (2000), Φ_Σ can then be written in a similar fashion as in (13):

$$\Phi_\Sigma(\mathbf{a}, \mathbf{b}) = \int_{\mathbf{a} < C\mathbf{y} \leq \mathbf{b}} \phi(y_1) \dots \phi(y_d) d\mathbf{y} = \int_{\tilde{a}_1}^{\tilde{b}_1} \phi(y_1) \dots \int_{\tilde{a}_r}^{\tilde{b}_r} \phi(y_r) dy_r \dots dy_1 \quad (28)$$

Note that the r -dimensional integral still has d active constraints: For variable l , the k_l constraints $\mathbf{a}_j < C_j^\top \mathbf{y} \leq \mathbf{b}_j$ for $j \in \{m_l + 1, \dots, m_{l+1}\}$ need to be satisfied simultaneously so that the limits in (28) are given by

$$\tilde{a}_l = \max_{m_l < i \leq m_{l+1}} \left\{ a_i - \sum_{j=1}^{l-1} C_{i,j} y_j \right\} \quad \text{and} \quad \tilde{b}_l = \min_{m_l < i \leq m_{l+1}} \left\{ b_i - \sum_{j=1}^{l-1} C_{i,j} y_j \right\}$$

for $l = 1, \dots, r$.

This idea can be generalized to singular normal variance mixtures. Proceeding as in Section 4.1 one obtains

$$F(\mathbf{a}, \mathbf{b}) = \int_{(0,1)^r} g(\mathbf{u}) d\mathbf{u}, \quad g(\mathbf{u}) = \prod_{l=1}^r (e_l(u_0, \dots, u_{l-1}) - d_l(u_0, \dots, u_{l-1}))$$

with

$$d_l(u_0, \dots, u_{l-1}) = \Phi \left(\max_{m_l < i \leq m_{l+1}} \left\{ \frac{a_i}{\sqrt{F_W^{\leftarrow}(u_0)}} - \sum_{j=1}^{l-1} C_{i,j} \Phi^{-1}(d_j + u_j(e_j - d_j)) \right\} \right),$$

$$e_l(u_0, \dots, u_{l-1}) = \Phi \left(\min_{m_l < i \leq m_{l+1}} \left\{ \frac{b_i}{\sqrt{F_W^{\leftarrow}(u_0)}} - \sum_{j=1}^{l-1} C_{i,j} \Phi^{-1}(d_j + u_j(e_j - d_j)) \right\} \right)$$

for $l = 1, \dots, r$. The RQMC methods described in Section 3 can be applied to the problem in this form to estimate $F(\mathbf{a}, \mathbf{b})$. The main difference is that the dimension of the problem in the singular case is given by the rank r as opposed to the dimension $d > r$ of the normal variance mixture.

B Gamma Mixture Models

For statistical purposes it is often interesting to study the distribution of the squared Mahalanobis distance of $\mathbf{X} \sim \text{NVM}_d(\boldsymbol{\mu}, \Sigma, F_W)$ given by $D^2(\mathbf{X}; \boldsymbol{\mu}, \Sigma) = (\mathbf{X} - \boldsymbol{\mu})^\top \Sigma^{-1}(\mathbf{X} - \boldsymbol{\mu})$. We write $D^2 := D^2(\mathbf{X}; \boldsymbol{\mu}, \Sigma)$ if there is no confusion.

It follows readily from the stochastic representation (1) of \mathbf{X} that, in distribution,

$$D^2 = W X^2$$

where $X^2 \sim \chi_d^2$. This immediately gives rise to a sampling algorithm to generate random variates from D^2 . Since a χ^2 distribution is a special case of a gamma distribution, it follows that $D^2 \mid W \sim \Gamma(d/2, 2W)$ where $\Gamma(\alpha, \beta)$ denotes a gamma distribution with shape $\alpha > 0$ and scale $\beta > 0$ which admits the density $f_{\Gamma(\alpha, \beta)}(x) = (\beta^\alpha \Gamma(\alpha))^{-1} x^{\alpha-1} e^{-x/\beta}$, $x > 0$, and distribution function $F_\Gamma(x; \alpha, \beta) = \int_0^x f_{\Gamma(\alpha, \beta)}(t) dt$ for $x > 0$. The function $\Gamma(z) = \int_0^\infty t^{z-1} e^{-t} dt$, $z > 0$ denotes the gamma function.

In the special case where $W = 1$ almost surely, $D^2 \sim \chi_d^2$; if W follows an inverse-gamma distribution so that \mathbf{X} follows a multivariate t with $\nu > 0$ degrees of freedom, it can be easily seen that $D^2/d \sim F(d, \nu)$. For the general case where only F_W^{\leftarrow} is available, we can use methods similar to the ones developed so far to approximate the density and the distribution function of D^2 .

Estimating the distribution function of D^2 Using a conditioning argument similar to the normal variance mixture case, we obtain that

$$F_{D^2}(x) = \mathbb{P}(D^2 \leq x) = \mathbb{E} \left(F_{\Gamma(d/2, 2)} \left(\frac{x}{W} \right) \right), \quad x \geq 0.$$

This univariate integral can be approximated directly using an RQMC approach similar to Algorithm 4.1. An implementation can be found in the function `pgammamix()` in the R package `nvmix`.

C Algorithms

Estimating the density function of D^2 In a similar fashion as in the derivation of Equation (3), the density of D^2 can be calculated as $f_{D^2}(x) = \int_0^1 \tilde{h}(u) du$ for $x > 0$, where

$$\tilde{h}(u) = \frac{1}{\Gamma(d/2)(2F_W^{\leftarrow}(u))^{d/2}} x^{d/2-1} \exp\left(-\frac{x}{2F_W^{\leftarrow}(u)}\right), \quad u \in (0, 1).$$

The functions \tilde{h} and h from Equation (17) differ only in constants with respect to u , the functional form is identical. Algorithm 5.2 can then, with some slight modifications, be used to estimate the density $f_{D^2}(x)$ (or $\log f_{D^2}(x)$); see also Remark 5.3. This is implemented in the function `dgrammix()` in the R package `nvmmix`.

Estimating the quantile function of D^2 Many applications, such as graphical goodness-of-fit assessment or random variate generation, rely on the quantile function of D^2 . Note that both the density and the distribution function of D^2 can be estimated as discussed above; the quantile function can then be estimated by numerically solving the equation $F_{D^2}(q_u) - u = 0$ for q_u where $u \in (0, 1)$ is given. We suggest using Newton's method: In iteration $k \geq 1$, given a current iterate $q_u^{(k)}$, the next iterate is given by

$$\begin{aligned} q_u^{(k+1)} &= q_u^{(k)} - \frac{F_{D^2}(q_u^{(k)}) - u}{f_{D^2}(q_u^{(k)})} \\ &= q_u^{(k)} - \text{sign}(F_{D^2}(q_u^{(k)}) - u_i) \exp\left\{\log\left(|F_{D^2}(q_u^{(k)}) - u_i|\right) - \log f_{D^2}(q_u^{(k)})\right\}. \end{aligned}$$

The second line is a numerically more stable version of the first. We remark that (potentially) many calls to $F_{D^2}(\cdot)$ and $f_{D^2}(\cdot)$ are necessary until convergence takes place. We also note that in most applications, the quantile function has to be evaluated at multiple inputs, say u_1, \dots, u_n . In order to reduce run time, one can sort the inputs u_i in increasing order and also store all calls to $F_{D^2}(\cdot)$ and $f_{D^2}(\cdot)$. These values can be used as starting values for the next quantile calculation. If they are reasonably close to the true quantile, the procedure enjoys local quadratic convergence so that only a few calls to $F_{D^2}(\cdot)$ and $f_{D^2}(\cdot)$ are needed. Furthermore, $F_{D^2}(\cdot)$ and $f_{D^2}(\cdot)$ can be estimated simultaneously using the same realizations of W , and all those realizations can also be stored so that they do not need to be generated more often than necessary. This is implemented in the function `qgrammix()` in the R package `nvmmix`; the same idea can be exploited to estimate the quantile function of univariate normal variance mixtures which is implemented in the function `qnvmix()`.

C Algorithms

Algorithm C.1 (RQMC Algorithm to estimate $\log \mu$ where $\mu = \int_{(0,1)^d} g(\mathbf{u}) d\mathbf{u}$.)

Given ε , B , n_0 , i_{\max} , estimate $\log \mu = \log(\int_{(0,1)^d} g(\mathbf{u}) d\mathbf{u})$ via:

- 1) Set $n = n_0$, $i = 1$, and compute $\hat{\mu}_{b,n,\log}^{\text{RQMC}} = \hat{\mu}_{b,0,n_0,\log}^{\text{RQMC}}$ for $b = 1, \dots, B$ and $\hat{\mu}_{n,\log}^{\text{RQMC}}$ from (11) and (12).

C Algorithms

- 2) Set $\hat{\varepsilon} = 3.5\hat{\sigma}_{\hat{\mu}_{n,\log}^{\text{RQMC}}}$ with $\hat{\sigma}_{\hat{\mu}_{n,\log}^{\text{RQMC}}}$ as in (10).
- 3) While $\hat{\varepsilon} > \varepsilon$ and $i \leq i_{\max}$ do:
 - 3.1) Set $n = n + n_0$, compute $\hat{\mu}_{b, in_0, (i+1)n_0, \log}^{\text{RQMC}}$, $b = 1, \dots, B$ and update $\hat{\mu}_{b, n, \log}^{\text{RQMC}} = -\log(i+1) + \text{LSE}(i\hat{\mu}_{b, n}^{\text{RQMC}}, \hat{\mu}_{b, in_0, (i+1)n_0}^{\text{RQMC}})$ for $b = 1, \dots, B$.
 - 3.2) Update $\hat{\mu}_{n, \log}^{\text{RQMC}} = -\log(B) + \text{LSE}(\hat{\mu}_{1, n, \log}^{\text{RQMC}}, \dots, \hat{\mu}_{B, n, \log}^{\text{RQMC}})$ and update $\hat{\varepsilon} = 3.5\hat{\sigma}_{\hat{\mu}_{n, \log}^{\text{RQMC}}}$.
 - 3.3) Set $i = i + 1$.
- 4) Return $\hat{\mu}_{n, \log}^{\text{RQMC}}$.

Algorithm C.2 (Variable reordering)

- 1) Start with given \mathbf{a}, \mathbf{b} and Σ .
- 2) Calculate or approximate $\mu_{\sqrt{W}} = \mathbb{E}(\sqrt{W})$.
- 3) a) Choose the first integration variable as

$$i = \underset{j \in \{1, \dots, d\}}{\text{argmin}} \left\{ \Phi \left(\frac{b_j}{\mu_{\sqrt{W}} \sqrt{\Sigma_{jj}}} \right) - \Phi \left(\frac{a_j}{\mu_{\sqrt{W}} \sqrt{\Sigma_{jj}}} \right) \right\}.$$

Swap components 1 and i of \mathbf{a} and \mathbf{b} and interchange both rows and columns of Σ corresponding to the variables i and 1.

- b) Update $C_{11} = \sqrt{\Sigma_{11}}$ and $C_{j1} = \Sigma_{j1}/C_{11}$ for $j = 1, \dots, d$. Set

$$y_1 = \frac{\int_{\hat{a}_1}^{\hat{b}_1} s \phi(s) ds}{\Phi(\hat{b}_1) - \Phi(\hat{a}_1)}$$

as expected value for u_1 , where

$$\hat{a}_1 = \frac{a_1}{\mu_{\sqrt{W}} C_{11}} \quad \text{and} \quad \hat{b}_1 = \frac{b_1}{\mu_{\sqrt{W}} C_{11}}.$$

This is the same as $\mathbb{E}(Z \mid Z \in [\hat{a}_1, \hat{b}_1])$ for $Z \sim N(0, 1)$.

- 4) For $j = 2, \dots, d$,
 - a) Choose the j th integration variable as

$$i = \underset{l \in \{j, \dots, d\}}{\text{argmin}} \left\{ \Phi \left(\frac{\frac{b_l}{\mu_{\sqrt{W}}} - \sum_{k=1}^{j-1} C_{lk} y_k}{\sqrt{\Sigma_{l,l} - \sum_{k=1}^{j-1} C_{lk}^2}} \right) - \Phi \left(\frac{\frac{a_l}{\mu_{\sqrt{W}}} - \sum_{k=1}^{j-1} C_{lk} y_k}{\sqrt{\Sigma_{l,l} - \sum_{k=1}^{j-1} C_{lk}^2}} \right) \right\}.$$

Swap components i and j of \mathbf{a} and \mathbf{b} and interchange both rows and columns of Σ corresponding to variables i and j and interchange rows i and j in C .

C Algorithms

- b) Update $C_{jj} = \sqrt{\Sigma_{jj} - \sum_{k=1}^{j-1} C_{jk}^2}$ and $C_{lj} = \frac{1}{C_{jj}} \left(\Sigma_{lj} - \sum_{k=1}^{j-1} C_{jk} C_{lk} \right)$ for $l = j + 1, \dots, d$ and set

$$y_j = \frac{\int_{\hat{a}_j}^{\hat{b}_j} s \phi(s) ds}{\Phi(\hat{b}_j) - \Phi(\hat{a}_j)}$$

where

$$\hat{a}_j = \frac{\frac{a_j}{\mu\sqrt{W}} - \sum_{k=1}^{j-1} C_{jk} y_k}{C_{jj}} \quad \text{and} \quad \hat{b}_j = \frac{\frac{b_j}{\mu\sqrt{W}} - \sum_{k=1}^{j-1} C_{jk} y_k}{C_{jj}}.$$

References

- Botev, Z. and L'Écuyer, P. (2015), Efficient probability estimation and simulation of the truncated multivariate student- t distribution, *Proceedings of the 2015 Winter Simulation Conference*, IEEE Press, 380–391, doi:10.1109/WSC.2015.7408180.
- Coffey, C. and Muller, K. (2000), Properties of doubly-truncated gamma variables, *Communications in Statistics-Theory and Methods*, 29(4), 851–857, doi:10.1080/03610920008832519.
- Cranley, R. and Patterson, T. (1976), Randomization of Number Theoretic Methods for Multiple Integration, *SIAM Journal on Numerical Analysis*, 13(6), 904–914, doi:10.1137/0713071.
- Eddelbuettel, D. (2012), Counting CRAN Package Depends, Imports and LinkingTo, <http://dirk.eddelbuettel.com/blog/2012/08/05/> (03/23/2013).
- Genz, A. (1992), Numerical Computation of Multivariate Normal Probabilities, *Journal of computational and graphical statistics*, 1(2), 141–149, doi:10.2307/1390838.
- Genz, A. and Bretz, F. (1999), Numerical computation of multivariate t -probabilities with application to power calculation of multiple contrasts, *Journal of Statistical Computation and Simulation*, 63(4), 103–117, doi:10.1080/00949659908811962.
- Genz, A. and Bretz, F. (2002), Comparison of methods for the computation of multivariate t probabilities, *Journal of Computational and Graphical Statistics*, 11(4), 950–971, doi:10.1198/106186002394.
- Genz, A. and Bretz, F. (2009), Computation of multivariate normal and t probabilities, vol. 195, Springer Science & Business Media, doi:10.1007/978-3-642-01689-9.
- Genz, A., Bretz, F., et al. (2019), mvtnorm: Multivariate Normal and t Distributions, R package version 1.0-11, <http://CRAN.R-project.org/package=mvtnorm>.
- Genz, A. and Kwong, K. (2000), Numerical evaluation of singular multivariate normal distributions, *Journal of Statistical Computation and Simulation*, 68(1), 1–21, doi:10.1080/00949650008812053.
- Gibson, G., Glasbey, C., and Elston, D. (1994), Monte Carlo evaluation of multivariate normal integrals and sensitivity to variate ordering, *Advances in Numerical Methods and Applications*, World Scientific Publishing, River Edge, 120–126.
- Glasserman, P. (2013), Monte Carlo methods in financial engineering, vol. 53, Springer Science & Business Media.
- Healy, M. (1968), Algorithm AS 6: Triangular decomposition of a symmetric matrix, *Journal of the Royal Statistical Society. Series C (Applied Statistics)*, 17(2), 195–197, doi:10.2307/2985687.
- Hickernell, F. and Hong, H. (1997), Computing multivariate normal probabilities using rank-1 lattice sequences, *Proceedings of the Workshop on Scientific Computing (Hong Kong)*, 209–215.
- Hofert, M., Hintz, E., and Lemieux, C. (2020), nvmix: Multivariate Normal Variance Mixtures, R package version 0.0-4, <https://CRAN.R-project.org/package=nvmix>.

References

- Hofert, M. and Hornik, K. (2016), qrmdata: Data Sets for Quantitative Risk Management Practice, R package version 2016-01-03-1, <https://CRAN.R-project.org/package=qrmdata>.
- Hofert, M. and Lemieux, C. (2019), qrng: (Randomized) Quasi-Random Number Generators, R package version 0.0-7, <https://CRAN.R-project.org/package=qrng>.
- Keast, P. (1973), Optimal parameters for multidimensional integration, *SIAM Journal on Numerical Analysis*, 10(5), 831–838, doi:10.1137/0710068.
- Kotz, S. and Nadarajah, S. (2004), Multivariate t Distributions and Their Applications, Cambridge University Press.
- Lemieux, C. (2009), Monte Carlo and Quasi-Monte Carlo Sampling, Springer, doi:10.1007/978-0-387-78165-5.
- Liu, C. and Rubin, D. (1994), The ECME algorithm: a simple extension of EM and ECM with faster monotone convergence, *Biometrika*, 81(4), 633–648, doi:<https://doi.org/10.1093/biomet/81.4.633>.
- Liu, C. and Rubin, D. (1995), ML estimation of the t distribution using EM and its extensions, ECM and ECME, *Statistica Sinica*, 19–39, doi:10.1006/jmva.1998.
- McNeil, A., Frey, R., and Embrechts, P. (2015), Quantitative Risk Management: Concepts, Techniques and Tools, Princeton University Press, doi:10.1007/s10687-017-0286-4.
- Mersmann, O. (2015), microbenchmark: Accurate Timing Functions, R package version 1.4-2.1, <http://CRAN.R-project.org/package=microbenchmark>.
- Nadarajah, S. and Kotz, S. (2008), Estimation methods for the multivariate t distribution, *Acta Applicandae Mathematicae*, 102(1), 99–118.
- Niederreiter, H. (1992), Random number generation and quasi-Monte Carlo methods, vol. 63, Siam.
- Owen, A. (2013), Better estimation of small Sobol’ sensitivity indices, *ACM Transactions on Modeling and Computer Simulation (TOMACS)*, 23(2), 11, doi:10.1145/2457459.2457460.
- Pfaff, B. and McNeil, A. (2016), QRM: Provides R-Language Code to Examine Quantitative Risk Management Concepts, R package version 0.4-13, <https://CRAN.R-project.org/package=QRM>.
- Pujol, G., Iooss, B., and Janon, A. (2017), sensitivity: Global Sensitivity Analysis of Model Outputs, R package version 1.15.0, <https://CRAN.R-project.org/package=sensitivity>.
- Rosenblatt, M. (1952), Remarks on a Multivariate Transformation, *The Annals of Mathematical Statistics*, 23(3), 470–472, doi:10.1214/aoms/1177729394.
- Sobol’, I. (1967), On the distribution of points in a cube and the approximate evaluation of integrals, *USSR Computational Mathematics and Mathematical Physics*, 7(4), 86–112, doi:10.1016/0041-5553(67)90144-9.
- Sobol’, I. (2001), Global Sensitivity Indices for Nonlinear Mathematical Models and their Monte Carlo Estimates, *Mathematics and computers in simulation*, 55(1-3), 271–280, doi:10.1016/S0378-4754(00)00270-6.

References

Wang, X. and Fang, K. (2003), The effective dimension and quasi-Monte Carlo integration, *Journal of Complexity*, 19(2), 101–124, doi:10.1016/S0885-064X(03)00003-7.